2009

Intelligent time-successive production modeling

Yasaman Khazaeni
West Virginia University

Intelligent Time-Successive Production Modeling

Yasaman Khazaeni

Thesis submitted to the
College of Engineering and Mineral Resources
at West Virginia University
in partial fulfillment of the requirements
for the degree of

Master of Science
in
Petroleum and Natural Gas Engineering

Approved by

Shahab D. Mohaghegh, PhD., Chair

Khashayar Aminian, PhD.

Razi Gaskari, PhD.

Grant Bromhal, PhD.

Department of Petroleum and Natural Gas Engineering

Morgantown, West Virginia

2009

Abstract

Intelligent time-Successive Production Modeling

Yasaman Khazaeni

A new framework is presented that uses production data history in order to build a field-wide performance prediction model. In this work artificial intelligence techniques and data driven modeling are utilized to perform a future production prediction for both synthetic and real field cases.

Production history is paired with geological information from the field to build large dataset containing the spatio-temporal dependencies amongst different wells. These spatio-temporal dependencies are addressed by information from Closest Offset Wells (COWs). This information includes geological characteristics (Spatial) and dynamic production data (Temporal) of all COWs.

Upon creation of the dataset, this framework calls for development of a series of single layer neural network, trained by back propagation algorithm. These networks are then fused together to form the "Intelligent Time-Successive Production Modeling"(ITSPM). Using only well log information along with production history of existing wells, this technique can provide performance predictions for new wells and initial hydrocarbon in place (IHIP) using a "volumetric-geostatical" method.

A synthetic oil reservoir is built and simulated using a commercial reservoir numerical simulation package. Production and well log data are extracted and converted to an all-inclusive dataset. Following the dataset generation several neural networks are trained and verified to predict different stages of production. ITSPM method is utilized to estimate the production profile for nine new wells in the reservoir. ITSPM is also applied to data from a real field. The field that is giant oil field in the Middle East includes more than 200 wells with forty years of production history. ITSPM's production predictions of the four newest wells in this reservoir are compared to real production data.

To Mom, Dad and Ali

Acknowledgments

First and foremost I wish to offer my sincerest gratitude to my supervisor, Dr Shahab Mohaghegh who has supported me throughout my thesis with his patience and knowledge whilst allowing me the room to work in my own way. I attribute the level of my Masters degree to his encouragement and effort and without him this thesis, too, would not have been completed or written. One simply could not wish for a better or friendlier supervisor.

I wish to thank my friends in MRB-135 whom I shared every moment of this work with. Without having the warmth and joyfulness we share in this office I would not be able to carry on with the hard work and finish this thesis. I also wish to thank all my friends; ones who have been beside me and ones who are distant, without their support studying all long days and nights far away from home would not be ever possible.

My gratitude also goes to Dr. Khashayar Aminian, Dr. Razi Gaskari, and Dr Grant Bromhal who kindly accepted to be a member of my thesis committee and all made significant contribution to this work through their generous comments.

Also, I would like to express my gratitude to Computer Modeling Group, for making the CMG reservoir simulator available to us to perform the reservoir simulations in this work.

And most importantly, I wish to thank my parents, although being oceans apart their fond love has certainly made this path much easier. They bore me, raised me, supported me, taught me, and loved me. To them I dedicate this thesis.

At the end I wish to thank dearly loved Ali, whom his presence defines the meaning of all these endeavors.

Contents

List of Figures

List of Tables

1. Introduction

Two of the most influential pieces of information in decision making and field developments are our depth of knowledge over the reservoir's state of depletion and remaining reserve estimation. This becomes more important in brown fields which most of wells are in their decline period and they can easily become non profitable if not drilled in the best spots.

There are several techniques enabling the reservoir engineers to have a reservoir model that is capable of predicting future behavior of the reservoir under different development strategies. These models are normally based on numerical solutions of the fluid flow equation and they require fairly accurate information about the formation and they are expensive considering the computational and human resources required building and using them.

In contrast, instead of lengthy and expensive numerical solutions, analytical solutions are simpler and cheaper. These solutions are normally limited to single well based analysis with many homogeneity assumptions. Although these solutions are much easier to develop and they do not need vast amount of data nor computer power, their deliverability is also limited.

Relying on availability of large amount of data about the field is not always a practical solution. Therefore the numerical solutions are not always practical. Also single well analysis techniques are not always good choices for field development strategy and decision makings.

Brown fields with marginal production rates or old fields without state-of-the-technology studies are not the best candidates for costly numerical simulation models. In some cases single well numerical models are built for some fields; these models limit the analysis to one well basis and don't give a full field understanding of the reservoir.

Beside these techniques, other empirical and data driven modeling techniques have always been a point of interest for reservoir engineers. One of the advantages of some of these methods is their ability to perform the analysis with a very limited amount of data (1) and (2). This advantage enables the reservoir engineer to have full field analysis for a field that has only production rate data with possibly some well logs are available to him.

Intelligent Time Successive Production Modeling (ITSPM) is a technique that uses production rate data from existing wells in the field along with any available well logs in order to build a field-wide well production model. Information from multiple wells are fused together and a spatiotemporal database is generated for the entire field. Artificial Intelligence and Neural Networks are used to infer a coherent model that is able to predict the existing and future well's production behavior.

By using geostatistics methods such as Ordinary Kriging the field properties information brought from well logs are mapped through the reservoir. This brings out the spatial dependencies throughout the reservoir and tries to employ these dependencies in predicting the future of the reservoir. The geostatistics application in this level of modeling also leads to a high resolution reserve estimation from the field.

2. Literature Review

In this literature review we try to present the basic underlying concepts of production data analysis techniques. Indeed this work is not a comprehensive evaluation of all the existing and methods and those being developed, but the intention is to gather the most dominant and influential works in this area.

These methods have been developed long ago and been in use for decades. Although most of them are single well-based analyses but they are powerful techniques and most of the time easy and cheap to implement.

After discussing the conventional production data analysis techniques a new method will be introduced which gathers and fuses single well analyses and tries to build a cohesive full field model capable of predicting the field's future behavior.

2.1. Production Data Analysis

From the time when oil and gas production started, the data taken from the wells production history appeared to be interesting for petroleum engineers. One of the reasons to analyze the production data is trying to predict the future production behavior of the oil and gas wells.

In most cases; a declining mode is present from the beginning of the production or after a somewhat constant production rate period in oil and gas wells. Analyzing this decline in production in petroleum engineering opened a topic called Declined Curve Analysis pioneered by Arps (3). Briefly Decline Curve Analysis is fitting the production data of a well or a field to a mathematical function to predict the performance of the well (or the field) up to an abandonment production rate.

In a complete empirical attempt Arps generated a set of rate-time decline curves that were considered as non-scientific. Arps decline equation is

$$q(t) = \frac{q_i}{(1 + bD_i t)^{\frac{1}{b}}}$$

In which D_i has an empirical equation as follows

$$D_i = \frac{q_i}{N_{pi}}$$

In above equation N_{pi} is the cumulative oil production for a period of time during which the reservoir pressure hypothetically decreases to 0 (psi).

Considering different values of b, different decline behaviors are categorized with $b = 0$ being exponential decline, $0 < b < 1$ hyperbolic decline and $b = 1$ a harmonic decline. Different values for b are also an indicator of the drive mechanism of the reservoir. (4)

So in a nutshell, production data decline curve analysis is a technique in which a theoretical model is fitted to the production rate data. This model will be able to predict the initial hydrocarbon in place and in some cases the formation properties.

Different analytical solutions were proposed for various conditions of the reservoir and drive mechanisms. In (5) the problem of Steady state water influx flow was addressed. After that and by using results from (6) Fetkovich suggested that for a water influx constant pressure producing well *q(t)* has the following form

$$q(t) = \frac{J_0(P_i - P_{wf})}{e^{\left(\frac{q_{i\ max}}{N_{pi}}\right)t}}$$

Where J_0 is the productivity index (STB/D/psi), P_{wf} is the bottom-hole flowing pressure (Psi) and $q_{i\,max}$ is the initial wide-open surface flow rate at $P_{wf} = 0$.

Also we know

$$q_i = J_0(P_i - P_{wf})$$

Where q_i is the initial surface rate at t=0 and

$J_0 = \frac{q_{i\,max}}{P_i}$.

Considering a wide-open decline where we have $P_{wf} = 0$ we will get to Arps' equation as

$$\frac{q(t)}{q_i} = e^{\frac{q_i}{N_{pi}}t}$$

According to this one can define $D_i = \frac{q_i}{N_{pi}}$. A dimensionless time factor is defined as

$$\mathrm{t_{Dd}} = \frac{q_i}{N_{pi}}\mathrm{t}$$

Assuming a circular reservoir and a pseudo-steady inflow Fetkovich suggested

$$q_i = \frac{kh(P_i)}{141.3\mu B(\ln\left(\frac{r_e}{r_w}\right) - 0.5)}$$

Total cumulative production can be defined in terms of reservoir variables

$$N_{pi} = \frac{\pi({r_e}^2 - {r_w}^2)\varphi c_t h P_i}{5.615B}$$

So the dimensionless time will become

$$t_{Dd} = \frac{\frac{0.00634kt}{\varphi\mu c_t {r_w}^2}}{0.5\left[(\frac{r_e}{r_w})^2 - 1\right]\left[\ln(\frac{r_e}{r_w}) - 0.5\right]}$$

And

$$q_{Dd} = \frac{q(t)}{\frac{kh(P_i)}{141.3\mu B(\ln\left(\frac{r_e}{r_w}\right) - 0.5)}}$$

Plotting q_{Dd} vs. t_{Dd} provides us with Fetkovich type curves shown in Figure 1

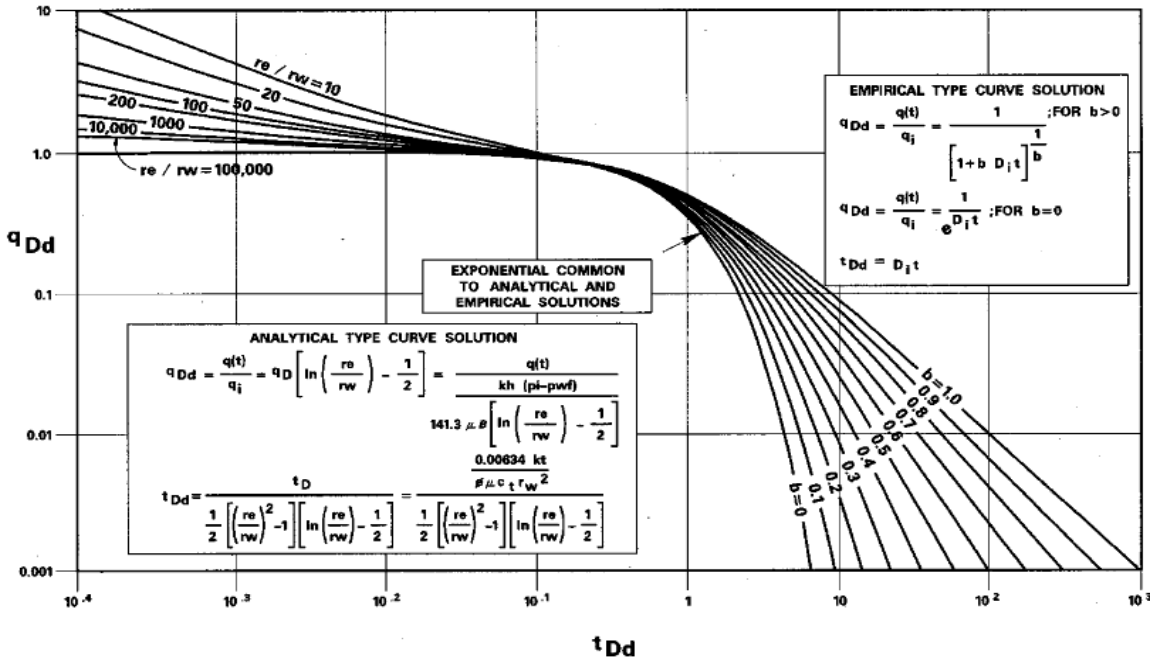

Figure 1 - Fetkovich Type Curves (7)

Merging the diffusivity equation solution under constant pressure flow with the Arps equation Fetkovich developed these single-type curves. One should keep in mind that in Fetkovich's approach anytime that the flow regime undergoes a new change like a shut-in or stimulation the values for q_i and P_i should be modified accordingly. (7)

In Fetkovich type curves compressibility of the gas is assumed to be almost constant or have small changes. Later on Carter (8) proposed a new method by taking into account for the changes in gas compressibility under high drawdown pressure producing conditions. In Carter's method a new parameter is defined as

$$\lambda = \frac{\mu(P_i)c_g(P_i)}{2} \quad \frac{[m(P_i) - m(P_w)]}{\left[(\frac{P}{Z})_i - (\frac{P}{Z})_w\right]}$$

For ideal gases $0.5 < \lambda < 1$, and for real gases values of λ can be less than 0.5; each value of λ will have a set of decline curves designed for that. A sample of these type

curves for $\lambda = 0.75$ is shown in Figure 2

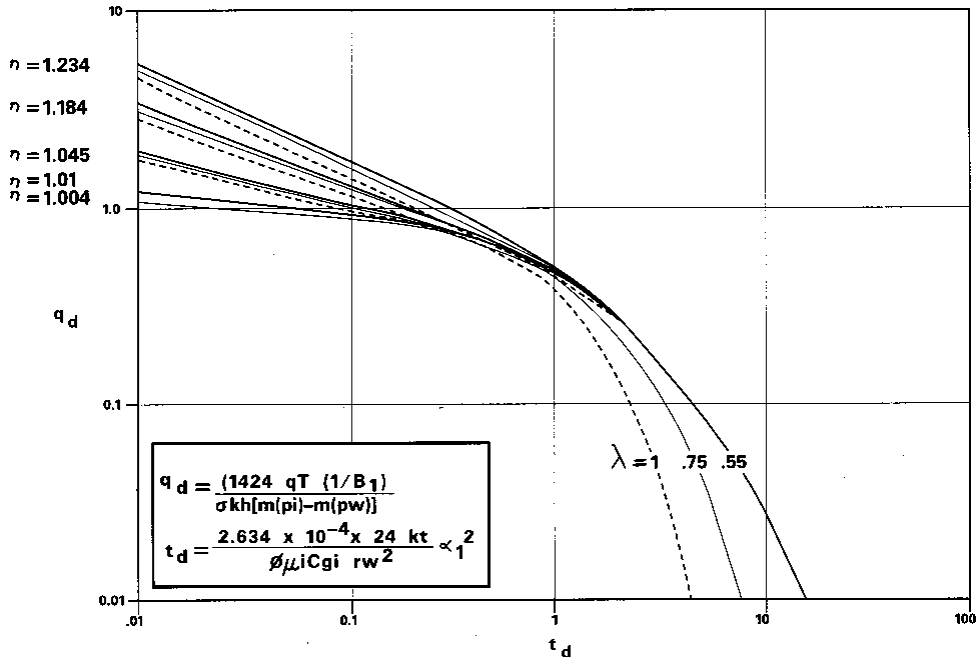

Figure 2 - Carter Type Curves

Later on, Fraim and Wattenbarger (9) brought the idea of using pseudo-time and pseudo-pressure to production decline analysis. Before that Agarwal (10) and Lee and Holditch (11) had used pseudo-time and pseudo-pressure in transient analysis of gas wells. In (9) it is shown that by using a normalized time as below. Decline curve for a closed real gas reservoir can always be expressed as an exponential decline (with b=0).

$$t_n = \int_0^t \frac{(\mu c_t)_i}{\mu(\bar{p})c_t(\bar{p})} dt$$

This normalized time is different from what was used in (11) and (10) because the fluid properties (viscosity and compressibility) are evaluated at average pressure rather than at the wellbore pressure which is the case in transient analysis's pseudo-time. Notice that the existence of μc_t in the integrand lets the normalized time have time dimension rather than be a non-dimensional parameter.

In a new theoretical approach, Palacio and Blasingame (12) surpassed some limitations in decline curve analysis previously existed techniques. The assumption of constant bottom-hole production condition was removed by this method. In (12), by using a material-balance time function, the authors suggested a solution which paved the way to minimizing the effect of changes in bottom-hole pressure. Material balance time in (12) is defined as

$$\bar{t} = \frac{N_p}{q_0}$$

Additionally a dimensionless time is also defined

$$\overline{t_{Dd}} = \frac{2\pi\left(\frac{.00634k}{\varphi\mu c_t A}\right)\bar{t}}{0.5Ln\left(\frac{4A}{e^{\gamma}C_A r_w^2}\right)}$$

Which together yield the following equation for the liquid decline,

$$\frac{q_0}{P_i - P_{wf}}\frac{141.2\mu B}{kh}\left[0.5Ln\left(\frac{4A}{e^{\gamma}C_A r_w^2}\right)\right] = \frac{1}{1+\overline{t_{Dd}}}$$

The difference between the Fetkovich's equation and Palacio and Blasingame's equation is that the latter uses the material balance time and the decline for liquid production in Blasingame equation is a harmonic decline.

For the gas production wells Palacio and Blasingame in (12) used the material balance pseudo-time with the real gas pseudo-pressure.

In gas well's production data analysis use of the pseudo-pressure is inevitable to account for the changes in gas compressibility and viscosity. This is more significant when well undergoes a large pressure change during its lifetime. (13)

Agarwal et. al. in (14) verified the material-balance time development from Palacio and Blasingame in (12). Using a single phase finite-difference reservoir simulator,

they verified that constant rate and constant bottom-hole pressure solutions for liquid and gas systems can be converted to an equivalent constant rate liquid solution.

An advancement of these new production decline-type curves over the previous works is that transient and boundary dominated flow periods are clearly distinguished. Other benefit is a better reserve estimation ability.

Another important contribution of Agarwal et. al. work (14) is the use of pressure derivatives in type curve analysis. This helps identifying the transition between the transient and pseudo-steady state flow regimes.

Cox et al (15) took Palacio and Blasingame's material balance time approach and used it with standard dimensionless variables. They showed that production data could be analyzed as an equivalent, constant-rate well test. This work is an example of combining constant-pressure decline curves with constant-rate pressure transient type curves.

Decline Curve Analysis, Type Curve Matching and all the cases discussed before are providing us with a single well studies. These methods do not provide us by a comprehensive analysis of the reservoir. If a field-wide complete model of the reservoir is needed for field performance prediction purposes, numerical simulation models that are history matched with available production data are the most desired method out there.

These models require lots of information about the field and the less data is available to build them the more uncertain they become. Therefore the history matching process would also become harder and sometimes close to impossible if not enough data is available. Considering the amount of man and computer power which should be available for the process of building a numerical simulation model for a field and history matching that model, this process would not prove to be economical for many mature fields. Adding to it the lack of field data for these fields it would not be a realistic choice at all.

There are some other field-wide modeling techniques that are not using numerical simulations. Gaskari and Mohaghegh in (16) proposed an integrated technique that uses fuzzy pattern recognition to come up with a full field analysis based on Decline Curve Analysis, Type Curve Matching and a single well history matching.

3. Methodology

In this section Intelligent Time Successive Production Modeling Technique is introduced and the procedure of implementing this technique is studied. This method, like other data-driven modeling methods (16) concentrates on field-production data history. The scheme, as will be described later, is using production rate at previous time steps (temporal dependency) and closest offset wells flow behavior (spatial dependency).

Spatial dependencies are a function of the degree of heterogeneity of the reservoir. The more heterogeneous the reservoir is, the more influential our knowledge of the spatial characteristics will be.

The heterogeneity in the reservoir characteristics are addressed by using a geostatistical estimation method throughout the reservoir. This tool honors the well logs characteristics information and generates a field-wide map through the entire reservoir for each geological characteristic. These maps can be used to accommodate the effect of heterogeneity by taking into account non-constant geological parameters around the wells, rather than assuming a unique value for each parameter.

After generating field-wide geological maps, different yard sticks are defined for building a dataset based on each well's production behavior at anytime. Geological characteristics and flow behavior along with the Euclidean distance between each well and its offsets are included in this data. The distance between wells and offsets can act as a measure of spatial dependencies between wells behavior. Also the age difference between wells and its offset wells is a measure of the influence each of the offset wells can have on the wells production performance.

Spatio-temporal dependencies of flow characteristics of different wells are modeled in a systematically integrated and cohesive manner. The resulting predictive model is employed to predict the future performance of the field. In this way a field-wide

comprehension of the reservoir is generated based on single well's performance history.

The method is applied to a synthetic numerical simulation model. This model is described in next sections. The only data which is used from simulation model would be the monthly production history along with reservoir characteristics information at well locations (Well Log Data).

Modeling is performed using neural networks as universal function Approximators. The related training and verification processes are also explained in much more detail later in this manuscript. At the end all these models are incorporated in a fully automatic prediction system which is called the Time-Successive Production Model. This tool will use the trained models to predict the field's production behavior for an extended time periods.

A brief flowchart of ITSPM method is illustrated in Figure 3.

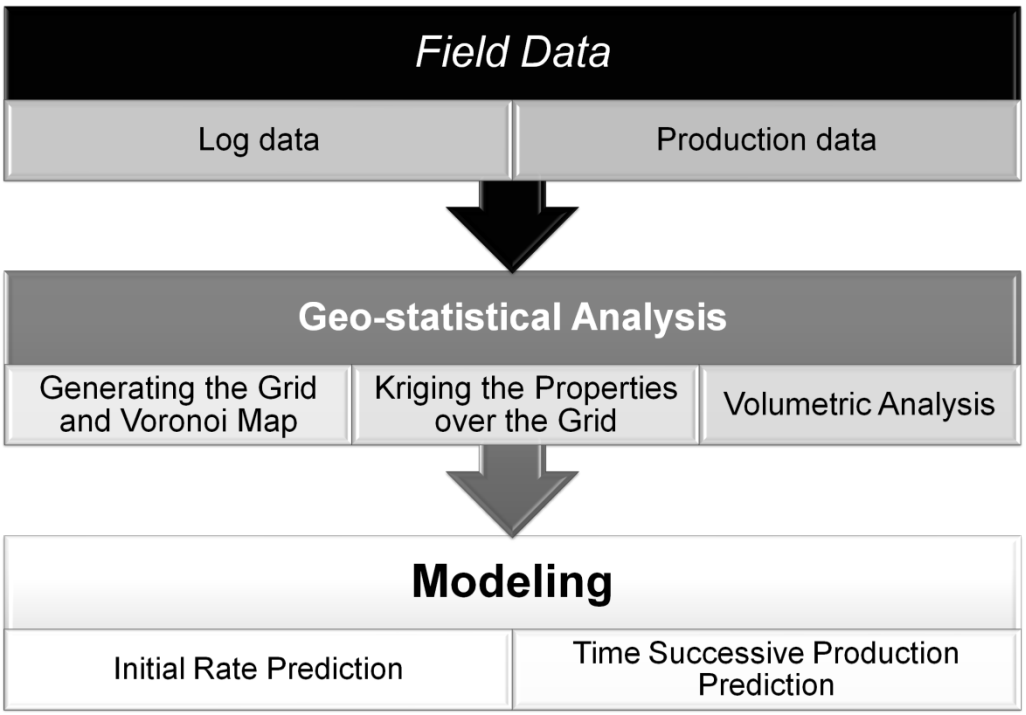

Figure 3 - Workflow of ITSPM

3.1. Reservoir Model Description

3.1.1. Structure and Properties

A commercial numerical simulation package was used to build a heterogeneous one layer, one phase (Oil) reservoir. The structure map and well locations are obtained from data related to a real reservoir. Other properties such as porosity, permeability and Initial water saturation maps are generated synthetically. These maps are built by using point values at a number of wells and creating the map by applying the Inverse Distance (17) method throughout the entire reservoir.

A structure map with well locations is shown in Figure 4. A 3D view of the reservoir structure and thickness shows the heterogeneity in these properties.

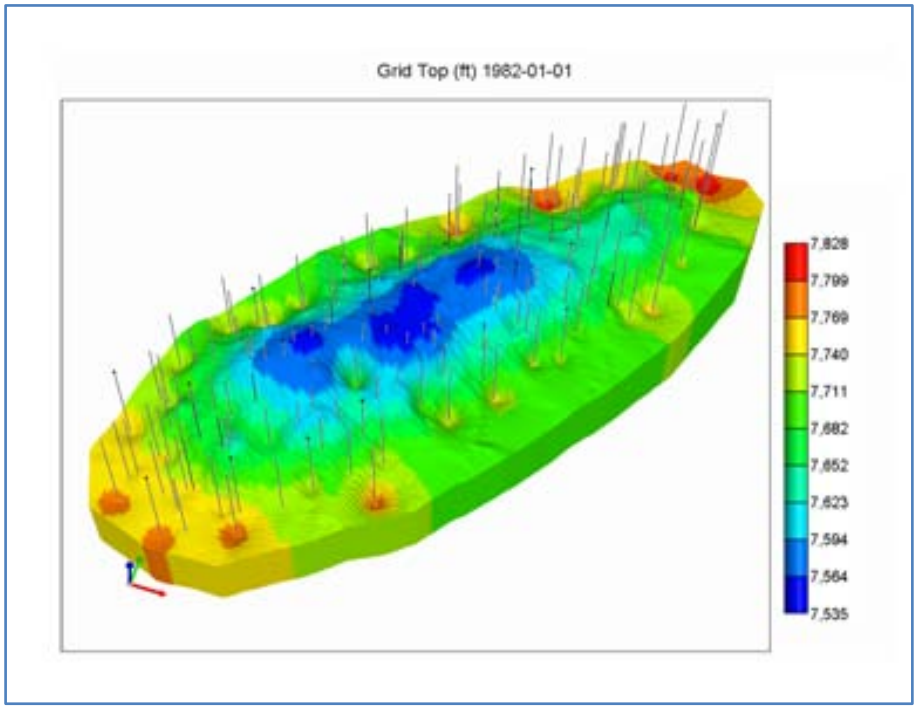

Figure 4 - 3D View of the Numerical Reservoir Model Structure

Property ranges within the reservoir is shown in Table 1. Also a full field map of porosity and permeability map that are used in this Model is included in Figure 5 and Figure 6.

Table 1 - Property Value Range in the Field

Property	Porosity	Net Thickness, ft	Permeability, mD	Initial Water Saturation	Formation Top, ft
Minimum	0.05	134.04	0.66	0.08	7537.19
Maximum	0.29	192.14	3.54	0.54	7819.38

A Cartesian grid system with an average grid size of 200 ft by 500 ft and total number of 10,000 grid blocks is used in the numerical simulator.

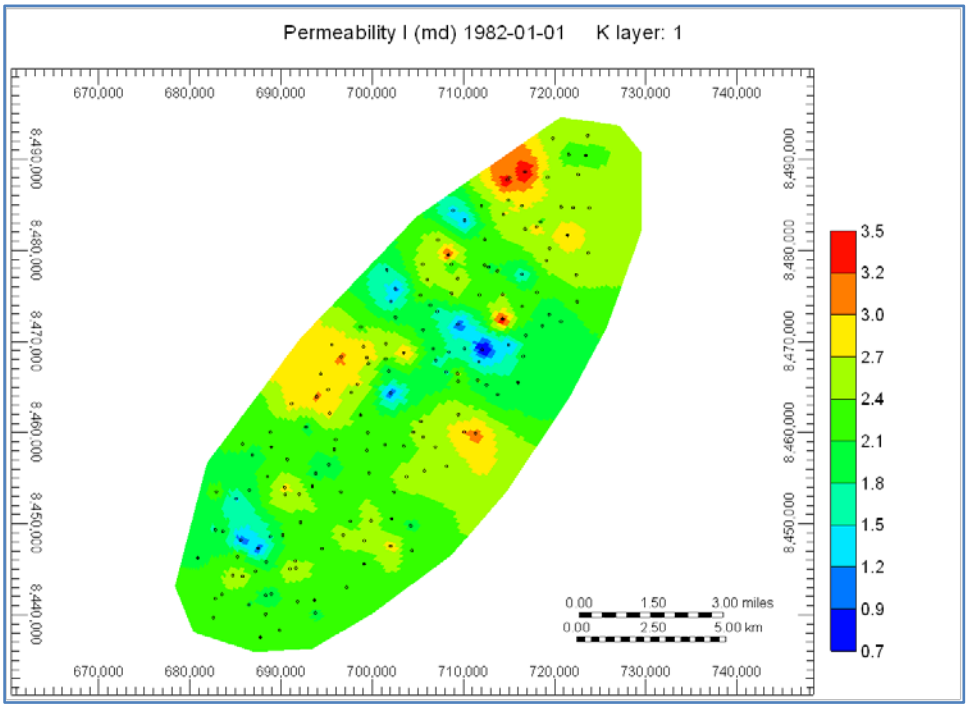

Figure 5 - Permeability Distribution in Numerical Model

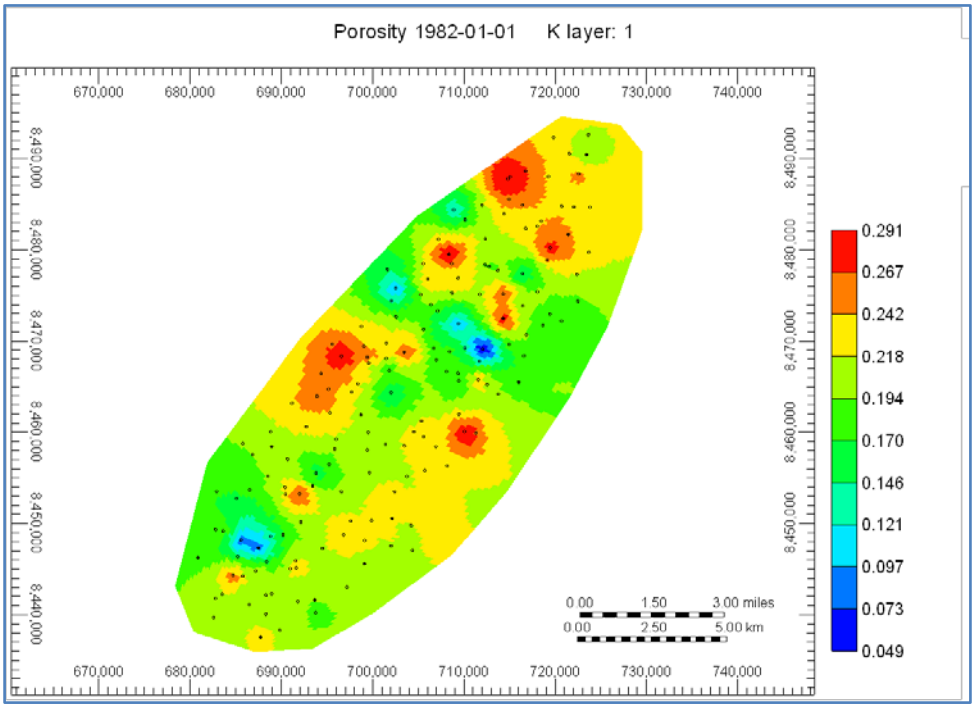

Figure 6 – Porosity Distribution in Numerical Model

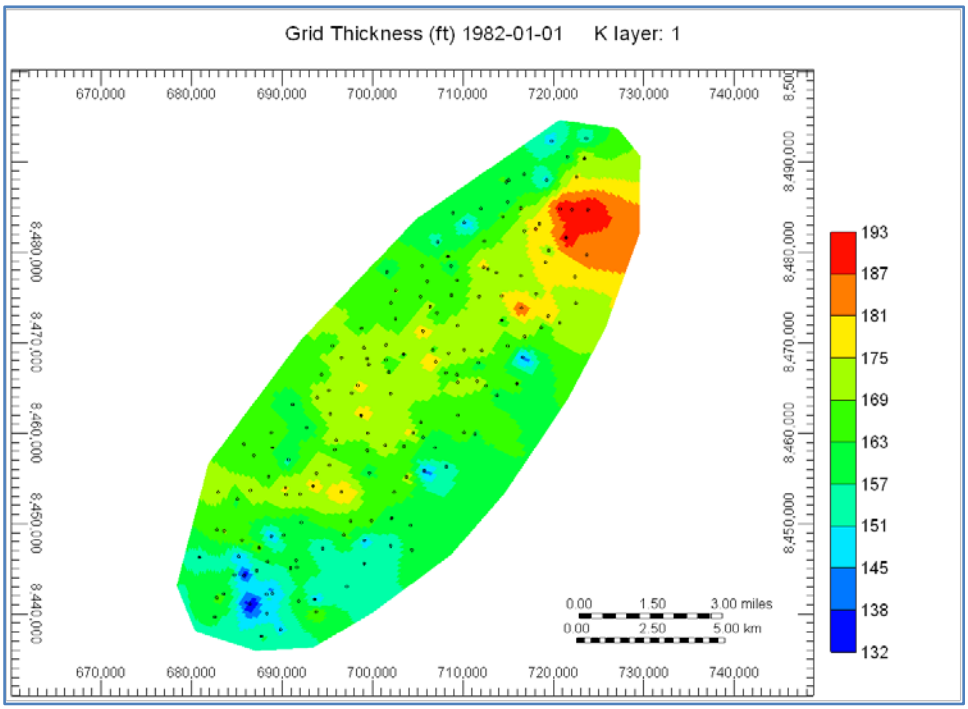

Figure 7 - Formation Thickness Distribution in Numerical Model

3.1.2. Well Configurations and Production Constraints

Production starts on January, 1982 and the field is put into production for 15 years. During 55 month 165 wells are drilled on a 3 well per month basis. While the initial pressure is equal to 4000 psi, All wells are producing on a constant bottom-hole pressure equal to 1500 psi and bubble point pressure is equal to 1000 psi therefore all the wells are producing oil and no free gas exist in the reservoir.

3.2. Single Well Modeling and Field-Wide Integration

Most of the production data analysis techniques as discussed in previous sections are single-well based. These methods do not have the ability to integrate the individual well performance assessments into a cohesive field-wide model. In this work our objective is to generate a workflow that can allow us to blend these single-well models into a field-wide comprehension of the reservoir.

First step is to define a boundary for each well. This is made possible by using the theory of image wells and the no-flow boundary creation between two wells. This theory implies that if two well starts producing at the same time at a distance of "*R*" with the same production rate. Assuming a homogenous formation the no-flow boundary will be created at the same distance to both wells.

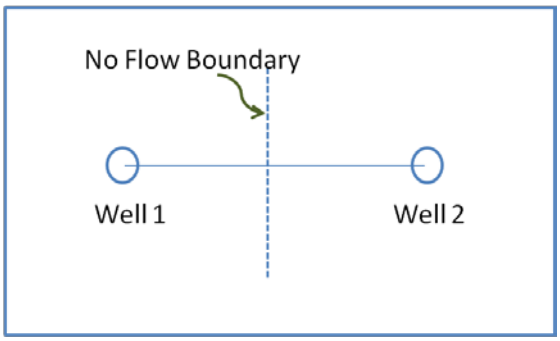

By using this definition and applying the Voronoi graph theory we delineate the reservoir to a number of Voronoi cells (equal to the number of wells). These Voronoi cells are considered as the Estimated Ultimate Drainage Area of each well.

3.2.1. Voronoi Delineation

By definition (18) the Voronoi cell of a point, $p \in S$, defined v_P, is the set of points x that are closer to p than to any other point in S. The union of the Voronoi cells of all generating points p in S forms the Voronoi diagram of S.

Using the well locations as the generating points, p and the reservoir boundaries as S. a Voronoi diagram is generated for S. This is done by a sweeping technique over the entire grid blocks. For each grid block the Euclidean distance of that block to all the wells are calculated, each block would belong to the Voronoi cell of the well which is closest to it. That well will be called the "*Parent well*" for that grid block. By sweeping all the blocks with this method the entire reservoir is delineated into different Voronoi cells that each one of them creates its own parent well's Estimated Ultimate Drainage Area (EUDA).This process is illustrated in Figure 8.

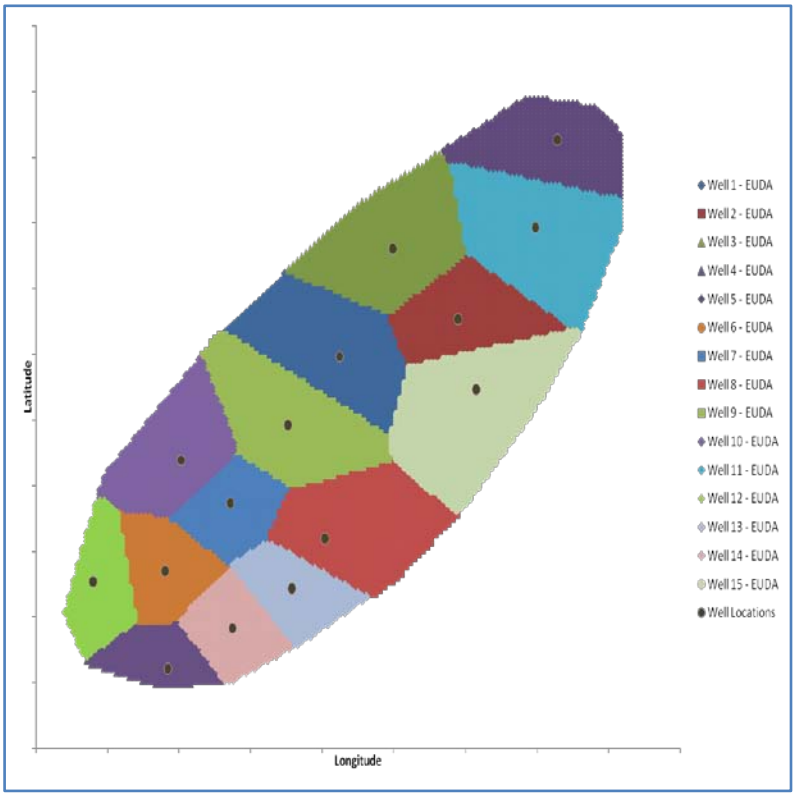

Figure 8 - Voronoi Delineation

These Voronoi cells are dynamic through the life time of the reservoir, meaning if a new well is drilled the ultimate drainage area for other wells shrink in a way so it accommodates the new well. This will continue as long as new wells are being drilled. Combining the information from closest offset wells and the dynamic value of EUDA at each time for any well, a coherent information platform is built for the entire reservoir.

3.3. Volumetric Analysis and Reserve Estimation

Initial Hydrocarbon in place estimation is carried out using a volumetric method. Not like most volumetric reserve estimation techniques that use single values for porosity and net pay, in this method these properties are estimated in the entire reservoir by geostatistical method of Ordinary Kriging using the values at well location.

3.3.1. Property Estimation

Assuming that properties like porosity, net pay and initial water saturation at well locations are known from well logs; these values can be used to generate a cohesive map for each property using Ordinary Kriging technique. The maps are generated for porosity and formation thickness and are compared to the real maps from the reservoir model. Porosity values estimated using the Ordinary Kriging technique is plotted and compared to the real porosity map in Figure 9. Same comparison for formation thickness values obtained from Ordinary Kriging is presented in Figure 10.

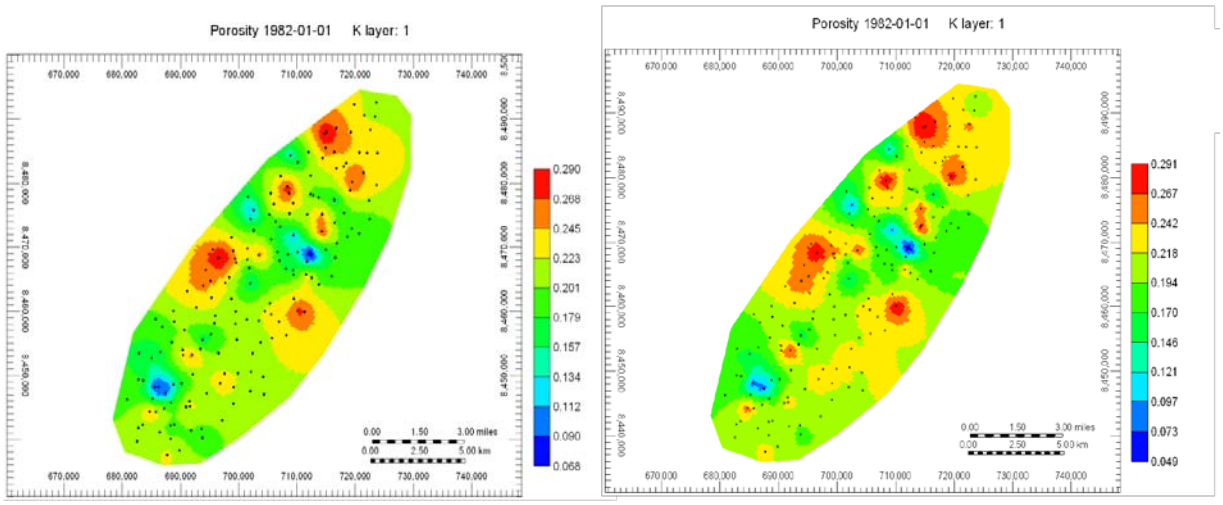

Figure 9 - Porosity Estimation Comparison - Geostatistics Result (Left) Real Map (Right)

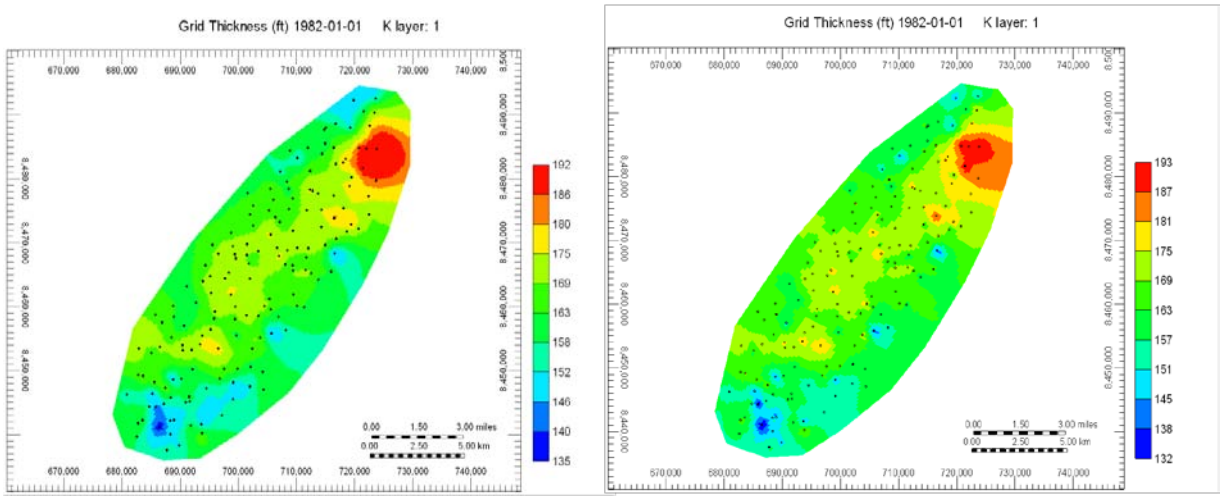

Figure 10 - - Formation Thickness Estimation Comparison - Geostatistics Result (Left) Real Map (Right)

For a detailed explanation on the geostatistical methods used in this work please refer to Appendix 1.

3.3.2. Volumetric Analysis

Two different volumetric analyses with different resolutions were performed to estimate the reserve in the field and both results were compared to the real initial reserve from the numerical simulation model.

Well Based Volumetric Analysis

In the well based analysis reservoir properties such as porosity, formation thickness and initial water saturation at each well is assigned to the whole Voronoi cell belonged to that well. In this case for each well's Voronoi cell total reserve estimation is calculated using

$$HC\ Pore\ volume\ (Rbbl) = 7758 * Area_{Voronoi\ Cell} * h_{Well} * \varphi_{Well} * (1 - S_{wi_{Well}})$$

These values are then added up to produce the total reserve estimate.

Grid Based Volumetric Analysis

In the geostatistical analysis which is performed to generate the grid-based values for each reservoir property is utilized to increase the accuracy of the estimate. Instead of assigning the well's property value to the entire drainage area, the reserve is estimated at each grid block using the property values for that block. Then the reserve is calculated with the same manner but this time the area should be the grid block's area.

$$HC\ Pore\ volume\ (Rbbl) = 7758 * Area_{Grid\ Block} * h_{Grid\ Block} * \varphi_{Grid\ Block} * (1 - S_{wi_{Grid\ Block}})$$

3.4. Production Data Assimilation

The production data by itself has a vast amount of information about the reservoir that has been infused to one value of production rate. Once it is comingled with the available static and dynamic information of the reservoir; it can bring out a cohesive full field model that represents the reservoir in a predictive system.

There are two different kinds of dependencies among the production data and reservoir characteristics. One is the spatial dependencies which are defined by the dependency of production rate to different properties in different locations of the reservoir. The second one is the temporal dependencies; involving the dependency of each well's performance to the history of the production of its own and other wells. In this work

we have tried to address these two issues with one predictive system. In order to do this a comprehensive dataset based on the reservoir characteristics and its production history is necessary.

3.4.1. Closest Offset Wells

Knowing the nature of the earth, in most cases one can assume that the closest the wells are the more similar their production behavior and characteristics will be. Using this fact in order to introduce the spatial and temporal dependencies we allocate the five Closest Offset Wells (COW) of each well and include their static and dynamic information in that well's data record.

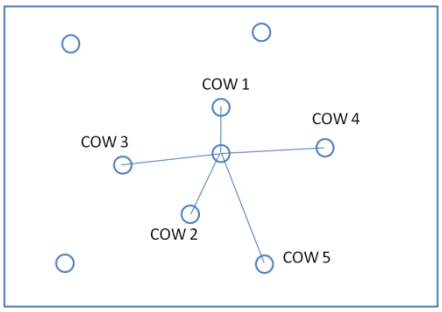

Figure 11- Closest Offset Wells Illustration

Data Set Structure

Production rate is recorded monthly, therefore at each month a new data record for each well is produced which includes the well's static information that doesn't change by time and its production information. Additional to this information the Closest Offset Wells' static information and their production data are also included in the data record. Also parameters such as distance between the well and offsets and the time difference between their production starting times is also included. This information is reflecting the significance of dependency between the production behavior of the offsets and the well.

Once the data set is generated for an enough length of time it is put into use to train a neural network which then learn to predict the well's production rate at next time step (month).

3.5. Neural Network Modeling

Training process of the neural networks is done in the Intelligent Data Evaluation and Analysis Environment (IDEA) (19). Data set is partitioned in three different segments. The first segment which is the largest of all three is used to train the network. In order to prevent the memorizing and over training effect in neural network training process, second segment of the data is taken for calibration. This part of the data is not introduced to the network for training but at each step of training the trained network is tested for this set and the best network is selected based on the calibration set prediction error.

Third segment of the data set is the verification part. This part is kept out of the training and calibration process and it is only used to test the precision of the network. Once a network is trained and calibrated, the final model is applied to the verification set. If the results are satisfactory the network is acceptable to be part of the entire prediction system.

3.6. Production Modeling and Prediction

3.6.1. Initial Rate Prediction Model

First step of production prediction is the initial production rate estimation. Once each new well is drilled and put into operation it shows an initial rate of production. This initial production rate depends on the characteristics of the reservoir at that location and also on the production history of the well surrounding it. The production history represents the state of the depletion of the reservoir. Integrating this information into the characteristics would lead to a better understanding of the future production behavior.

In a mature field that the reservoir has been producing for a long time and been depleted at most locations, new well's initial production rate not only depends on the location's characteristics but it is a function of the well's production starting time; the later the well is drilled the less the initial rate may be.

During the reservoir life span, at each time that a new well is drilled, the entire well's information can be a new instance of these dependencies. In order to utilize this information and infuse it into a predictive model, its initial rate and characteristics along with the dynamic and static information from its offset wells is recorded right after drilling is complete. This data assimilation leads into a data set that is used to train our first neural network model.

The first predictive model which is trained, calibrated and verified to predict the initial production rate of new well's is designed using a dataset built based on the production history of the numerical reservoir model, described in previous sections. First 156 wells out of a total number of 165 wells are considered to be existing wells while the dataset is built during a 5 years' time frame. 156 data records is built each representing one well at their initial production time. A complete list of inputs that are included in the dataset is reviewed in Table 2.

Table 2 - Initial Production Rate Prediction Model Input List

Input Data			
Well's		**Closest Offset Wells'**	
Static Information	Porosity	**Static Information**	Porosity
	Formation Thickness		Formation Thickness
	Initial Water Saturation		Initial Water Saturation
	Formation Top		Formation Top
	Location's Lat and Long	**Dynamic Information**	Estimated Ultimate Drainage Area
Dynamic Information	Estimated Ultimate Drainage Area		Initial Production Rate
			Current Production Rate
		Relative Information	Time Difference in Date of first Production
			Distance to the Well

Out of these input parameters not all are used to train the neural network. A Key Performance Indicator process is performed to rank the most influential input parameters on the Initial Production Rate.

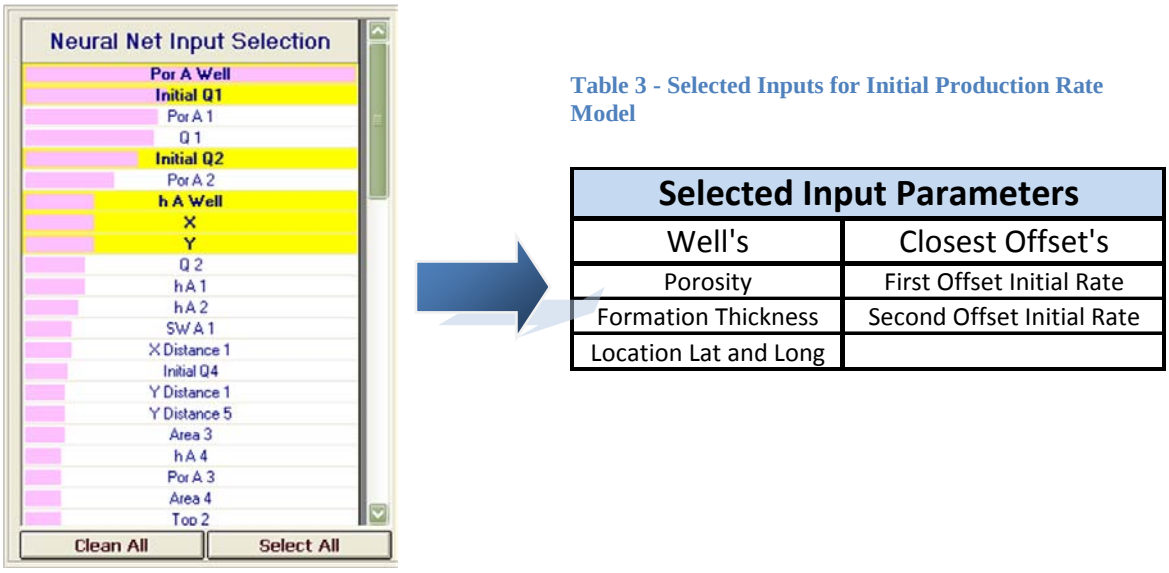

Table 3 - Selected Inputs for Initial Production Rate Model

Selected Input Parameters	
Well's	Closest Offset's
Porosity	First Offset Initial Rate
Formation Thickness	Second Offset Initial Rate
Location Lat and Long	

Figure 12 - Key Performance Indicator

Neural Network's design and data allocation is described in Table 4

Table 4 - Initial Rate Prediction Network Design and Data Allocation

Networks Training Method	Number of Hidden Layers	Number of Hidden Neurons	Number of Data Records	Training Data (%)	Calibration Data (%)	Verification Data (%)
Back Propagation	1	14	156	80%	10%	10%

It should be noted that the verification data set is different from the other 9 new wells that are kept completely out of networks dataset. Once the neural network is verified it will be applied to the new wells to predict the initial production rate.

3.6.2. Production Profile Prediction Model

After estimating the initial production rate for a new well, the production rate is modeled in a time successive fashion. In other words at each time step, the production rate is predicted based on previous production rates and offset wells' information.

In order to have a more accurate prediction at each time, we decided to use the past three months' production rates as input values for the neural network. This can be applied for modeling the production at month four through.

Three Separate neural networks are designed to predict different stages of the production profile. The initial decline of the production, however need a different strategy to be modeled than the tail of the production.

3.6.3. Second and Third Month Models:

In second and third month of production we do not have the privilege of using the last three months production rates as input values simply because the well has not been producing for three months. In this case two specific neural networks are trained, calibrated and verified to predict the second and third month of production. In these two networks respectively last one and two month of production is used as input values.

Input parameters for the second month production model are presented in Table 5. The only additional input from the First model (Initial Rate Prediction) is the initial

production rate of the well which is now available and can be used for prediction of the second time step.

Table 5 - Second Month Production Rate Prediction Model Input List

Input Data			
Well's		**Closest Offset Wells'**	
Static Information	Porosity	**Static Information**	Porosity
	Formation Thickness		Formation Thickness
	Initial Water Saturation		Initial Water Saturation
	Formation Top		Formation Top
	Location's Lat and Long	**Dynamic Information**	Estimated Ultimate Drainage Area
Dynamic Information	Estimated Ultimate Drainage Area		Initial Production Rate
	Initial Production Rate		Current Production Rate
		Relative Information	Time Difference in Date of first Production
			Distance to the Well

Same as previous model, not all of these input parameters are used to train the neural network. A Key Performance Indicator process is performed and most influential inputs are selected.

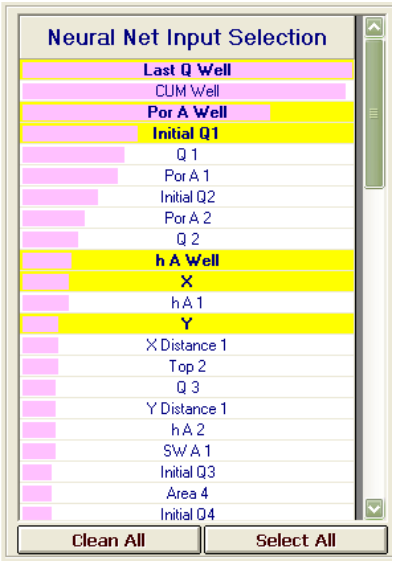

Table 6 - Selected Input for Second Month Production Rate Model

Selected Input Parameters	
Well's	Closest Offset's
Porosity	First Offset Initial Rate
Formation Thickness	
Location Lat and Long	
Initial Production Rate	

Figure 13 - Key Performance Indicator

The design of the neural network and data partitions are shown in Table 7.

Table 7 - Second Month Rate Prediction Network Design and Data Allocation

Networks Training Method	Number of Hidden Layers	Number of Hidden Neurons	Number of Data Records	Training Data (%)	Calibration Data (%)	Verification Data (%)
Back Propagation	1	15	153	80%	10%	10%

It should be noted same as in Initial rate prediction model, 9 new wells and 3 wells that did not have their second month production available in the training data are kept completely out of networks dataset. Once the neural network is verified it will be applied to the new wells to predict the second month production rate.

Input parameters for the Third month production model are presented in Table 8. The only difference with inputs from the Second Month Model is that now two previous production rates will be introduced as input values to the network.

Table 8 - Third Month Production Rate Prediction Model Input List

Input Data			
Well's		**Closest Offset Wells'**	
Static Information	Porosity	**Static Information**	Porosity
	Formation Thickness		Formation Thickness
	Initial Water Saturation		Initial Water Saturation
	Formation Top		Formation Top
	Location's Lat and Long	**Dynamic Information**	Estimated Ultimate Drainage Area
Dynamic Information	Estimated Ultimate Drainage Area		Initial Production Rate
	Initial Production Rate		Current Production Rate
	Second Month Production Rate	**Relative Information**	Time Difference in Date of first Production
			Distance to the Well

With the same procedure that was explained in previous network designs, most influential input parameters were selected for training this network and are shown in Table 9.

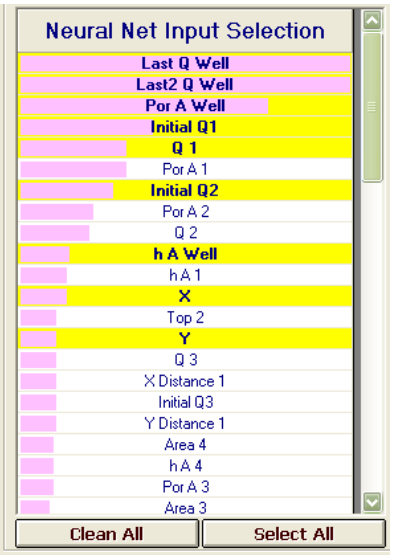

Table 9 - Selected Input for Third Month Production Rate Model

Selected Input Parameters	
Well's	Closest Offset's
Porosity	First Offset Initial Rate
Formation Thickness	First Offset Current Production Rate
Location Lat and Long	Second Offset Initial Rate
Initial Production Rate	
Second Month Production Rate	

Figure 14 - Key Performance Indicator

For the third month production rate prediction model, the network design and data partitions are shown in Table 10.

Table 10 - Third Month Production Rate- Network Design and Data Allocation

Networks Training Method	Number of Hidden Layers	Number of Hidden Neurons	Number of Data Records	Training Data (%)	Calibration Data (%)	Verification Data (%)
Back Propagation	1	17	150	80%	10%	10%

Same as in previous networks, 9 new wells and 6 wells that did not have their third month production available in the training data are kept completely out of networks dataset. Once the neural network is verified it will be applied to the new wells to predict the third month production rate.

3.6.4. Forth Month and after Production Model (Tail Model):

Once we are done with the initiation time steps prediction, an inclusive neural network is trained for modeling every step of the production profile based on last three months production and closest offset wells' real time information.

A list of available inputs for this model is presented in Table 11.

Table 11 - Production Tail Model Input List

Input Data			
Well's		**Closest Offset Wells'**	
Static Information	Porosity	**Static Information**	Porosity
	Formation Thickness		Formation Thickness
	Initial Water Saturation		Initial Water Saturation
	Formation Top		Formation Top
	Location's Lat and Long	**Dynamic Information**	Estimated Ultimate Drainage Area
Dynamic Information	Estimated Ultimate Drainage Area		Initial Production Rate
	Initial Production Rate		Current Production Rate
	Production at 3 months ago	**Relative Information**	Time Difference in Date of first Production
	Production at 2 months ago		Distance to the Well
	Production at 1 months ago		

One significant difference between this model and previous three models is in the definition of the output parameter. All previous models use production rate as the output. In the forth model, however, to attain more robust and accurate results, output parameter is defined to be the change in production rate from the last month production. This output selection has a considerable effect on the final result of production profile prediction.

Had production rate be selected as output, sometimes due to small changes of rate in the production tail, an increase in rate would be observed in the models' result instead of a decline. Consequences of this error would be a poor production profile prediction. Selecting ΔQ as the output guarantees a decline in rate no matter how small this change might be. Therefore it improves the ability of the predictive model in predicting the tail of the production.

Again by using Key Performance Indicator the most influential input parameters are selected in training the network.

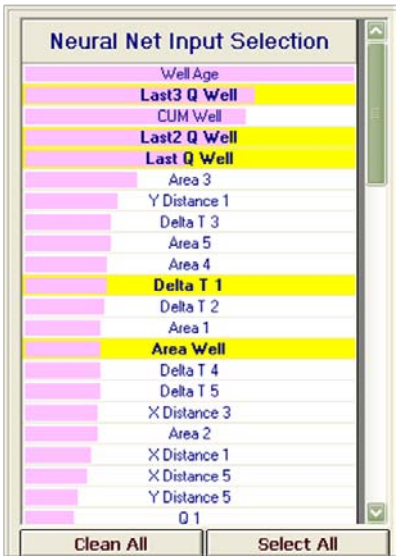

Figure 15 - Key Performance Indicator

Table 12 - Selected Input for Production Tail Model

Selected Input Parameters	
Well's	Closest Offset's
Porosity	First Offset's Time Difference in Date of first Production
Formation Thickness	
Estimated Ultimate Drainage Area	
Location Lat and Long	
Initial Production Rate	
Production at 3 months ago	
Production at 2 months ago	
Production at 1 months ago	

Networks data allocation and the structure of the network is shown in Table 13

Table 13 - Production Tail Model - Network Design and Data Allocation

Networks Training Method	Number of Hidden Layers	Number of Hidden Neurons	Number of Data Records	Training Data (%)	Calibration Data (%)	Verification Data (%)
Back Propagation	1	64	5745	60%	20%	20%

3.6.5. Intelligent Time Successive Production Model

Once all the four models are trained and verified it's the time to put them together in an integrated system that is capable of predicting the entire field's production. We are calling this integrated system a time-successive model because its prediction at each time depends on the previous time steps predictions.

Time Successive model is tested on the same simulation model which was discussed before. At the beginning of the year 1987 the last set of production data for 156 wells is obtained from the simulator. This set of data is used to initialize the ITSPM. At each time step depending on the state of the well one of the four designed models are used to predict its next time step production rate. At each time step all the wells are swept and their production is predicted and recorded in the next step rates vector. If at any

time a new well is drilled using the initial rate prediction model, its initial rate is predicted and the well is added to the list of the producing wells. Because after the first step systems' inputs are generated based on the previous step's outputs, model is completely independent from the simulation models' result.

It should be noted that closest offset wells are determined dynamically, meaning that during the reservoir's lifetime that new wells are added to the reservoir each well's offset wells are changing. In order to address this offset wells for each well are recalculated at each time step.

Implementing this step is done in Visual Basic environment. A controller program is designed and tested. Program uses the verified neural networks' as .dll files. These files are called inside the program at each time step for each well depending on which one fits the wells' state of production.

3.7. Sensitivity Analysis

In the previous section we pointed out the dependency of each step's output to its previous step's outcome. Now in order to have a quantified understanding of this dependency a sensitivity analysis is performed.

By exposing a determined error to the initial rate prediction model, results of ITSPM are regenerated and the final error is observed. As long as the output of ITSPM would not diverge from the desired outcome by an extremely high error we can make sure that by performing a Montecarlo analyses on uncertain Initial rate predictions a well defined range of production profile might be predicted for the entire wells.

Same study can be performed to understand the sensitivity of the final results to reservoir characteristics information. This procedure was conducted to study the final results' dependency on porosity data precision.

Other characteristics and input data information also can undergo a sensitivity analysis. The uncertain nature of our knowledge about reservoir characteristics and the

noisy production data will always bring down the precision of our predictions for future. At the end the more robust our prediction method is the less sensitive it will be to the errors and uncertainties associated with the data.

3.8. Time Successive Production Prediction of a Real Reservoir

In order to examine the validity of this technique, it's applicability to a real case is studied. The method was applied on a giant oil field production data history. An over 40 years of production data and reservoir characteristics at well locations is available.

This field has 210 oil producing wells. Wells are drilled from 1963 to 2001. The wells location and Estimated Ultimate Drainage Area which is assigned to them by Voronoi technique is shown in Figure 16.

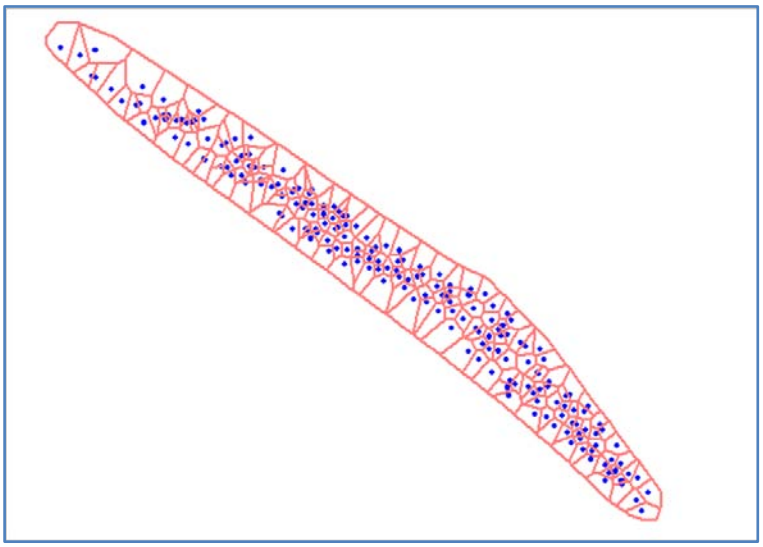

Figure 16 - Real Field Wells and Estimated Ultimate Drainage Area

Available static information about this field includes porosity and formation net pay at the wells. Also permeability value obtained from well tests and flowing bottom-hole pressure are also available. Initial pressure of the reservoir is 4,437 Psia and initial temperature is 190 F.

Ranges for these parameters are shown in Table 14.

Table 14 - Real Data Property Value Ranges

Property	Porosity %	Net Thickness, ft	Permeability, mD	Initial Oil Saturation %	Flowing Bottom-Hole Pressure, Psia
Minimum	10.00	170.56	3.04	63.00	1500.00
Maximum	21.00	3462.37	4679.00	83.00	4079.00

As it comes by its nature, production data contains a lot of noise and uncertainty. To overcome this noise before we use the data in Time Successive prediction method, for each well Decline Curve Analysis is performed and the decline curve data replace real production data, a sample of these decline curves is shown in Figure 17 - Decline Curve Fitted to the Production Data (Blue Solid) – Production Data (Green dots).

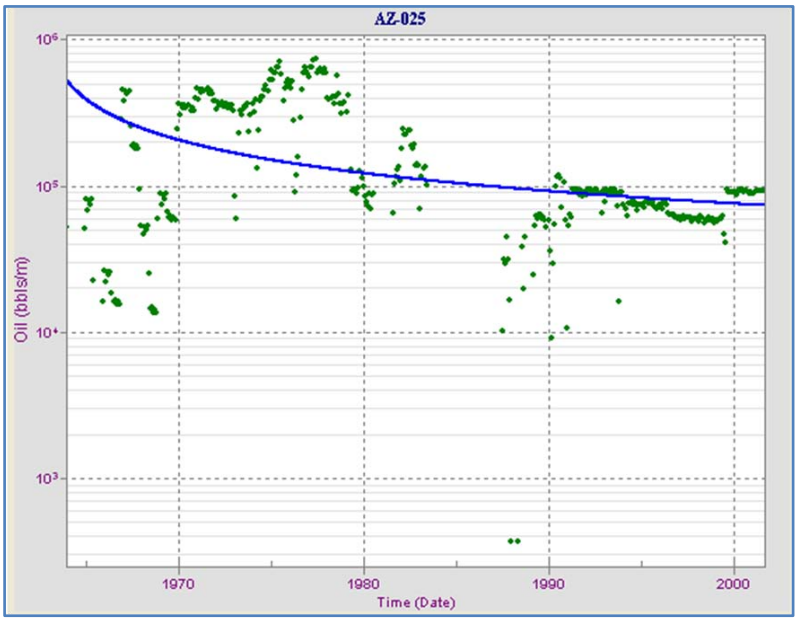

Figure 17 - Decline Curve Fitted to the Production Data (Blue Solid) – Production Data (Green dots)

Out of 210 wells that are producing in the field 4 youngest wells which are drilled in 2001 are taken out for verification purpose. The dataset is built based on 206 wells information and oil production data. Dataset generation follows the same path as described in previous section. Five Closest Offset Wells are located and their information is included in the dataset.

Looking at the initial rate of production of the 206 existing wells a declining trend during the life time of the reservoir is apparent. This can be explained as a result of the

depleting the reservoir during over 40 years of production. Due to this decreasing trend the initial rate of the new wells would be more correlated to the latest existing wells rather than the older ones. To address this issue of depletion, the last 20 years of production data was used to model the initial rate of production.

In the first model a neural network is trained using back propagation technique selected inputs are shown in Table 15. The dataset structure is the same as what was explained in Initial Rate Prediction Model in previous section.

Table 15 – Initial Production Rate Prediction Model - Input List

Selected Input Parameters	
Well's	Closest Offset's
Formation Thickness	First Offset Initial Rate
Initial Oil Saturation	Second Offset Initial Rate
Location Lat and Long	Forth Offset Initial Rate
Date of First Production	First Offset Time Difference in Date of first Production
	Second Offset Time Difference in Date of first Production
	Distance to First Offset Well
	Distance to Second Offset Well
	First Offset Well's Current Production Rate
	Second Offset Well's Current Production Rate

For second and third month of the production two separate models are designed and two neural networks are trained and verified. Not like the synthetic model case, the output of these neural networks is the cumulative production rather than the rate at each time step. The cumulative production seemed to be a better choice for prediction because of its less noisy behavior and always increasing nature. In the second month cumulative production prediction model the previous month cumulative is used as an input and for the third month two preceding month data are used as inputs. Networks

selected inputs are shown in Table 16 and. These inputs are selected based on a key performance indicator analysis.

Table 16 - Second Month Cumulative Prediction Model - Input List

Selected Input Parameters	
Well's	Closest Offset's
Formation Thickness	Forth Offset Initial Rate
Initial Oil Saturation	Third Offset Cumulative Production
Porosity	First Offset Time Difference in Date of first Production
Flowing Bottom-hole Pressure	Second Offset Time Difference in Date of first Production
Initial Production Rate	Third Offset Time Difference in Date of first Production
Date of First Production	Distance to First Offset Well
	Distance to Second Offset Well
	Distance to Third Offset Well
	First Offset Well's Current Production Rate
	Second Offset Well's Current Production Rate
	Third Offset Well's Current Production Rate

Table 17 - Third Month Cumulative Prediction Model - Input List

Selected Input Parameters	
Well's	Closest Offset's
Initial Oil Saturation	Forth Offset Initial Rate
Initial Production Rate	First Offset Time Difference in Date of first Production
Second Month Production Rate	Second Offset Time Difference in Date of first Production
Date of First Production	Distance to First Offset Well
	Second Offset Well's Current Production Rate
	Fifth Offset Well Estimated Ultimate Drainage Area

Once these three networks are trained and verified, next step is to predict the cumulative production for the rest of wells life time. This is done by using a three month window of past cumulative production value as inputs along with the reservoir characteristics and offset wells information. Because of the depletion in the reservoir, recently drilled wells experience a lower value of cumulative production compare to the older ones within the same length of time. To be able to predict the younger wells with lower cumulative production values most recent 91 wells information were used so high values of cumulative at beginning of the reservoir life time would not mislead the training process. This step's neural network's input parameters are shown in Table 18.

Table 18 - Cumulative Production Prediction Model - Input List

Selected Input Parameters	
Well's	Closest Offset's
Porosity	First Offset Well's Porosity
Initial Oil Saturation	Second Offset Well's Porosity
Formation Thickness	Forth Offset Initial Decline Rate
Permeability (Well Test Result)	
Well's Location Lat and Long	
Initial Oil Saturation	
Initial Production Rate	
Three preceding Months' Cumulative Production	
Date of First Production	

Now that all models are trained and verified they can be used in the Time Successive Prediction. Last 4 wells were taken out of all the dataset so they can be used to verify the results of this prediction technique. The comparison of their actual cumulative production (decline curve) and Time successive prediction results are demonstrated in results section.

4. Results

In this section we present the outcomes of applying this technique to the numerical simulation model production history information which was introduced before.

4.1. Volumetric Analysis Results

As expressed before the initial oil in place was estimated using a geostatistical volumetric method. Two separate analysis was performed one by assuming that all 165 wells have well log information and second by assuming only less than 30 % of the wells (48 wells) have well information available. Results of both analyses were then compared to the actual value of Initial Oil In Place from the numerical simulator model.

Distribution of the 48 wells among the 165 well is shown in Figure 18.

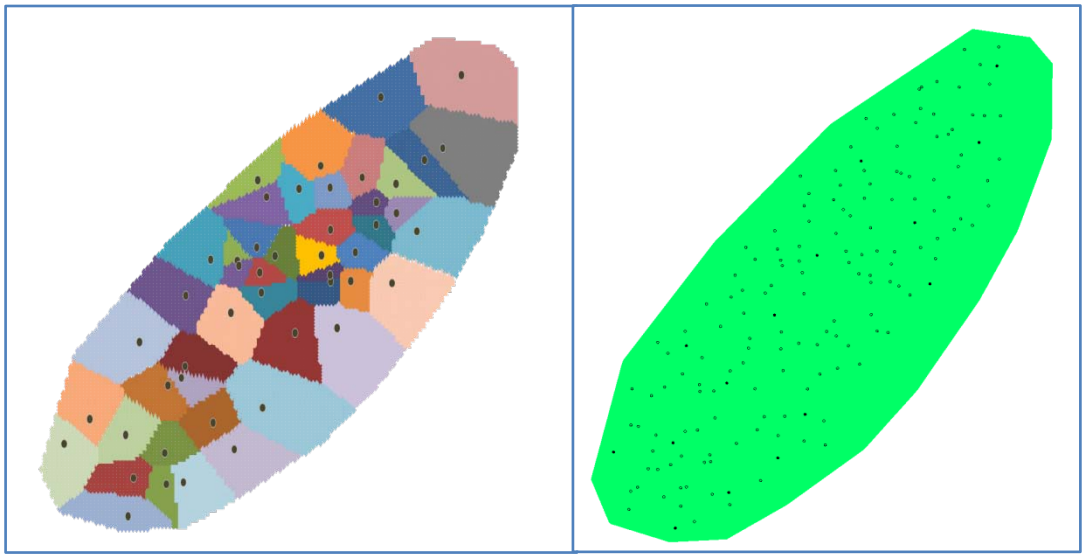

Figure 18 - Distribution of 30% Selected Well Logs

Results of these analyses are presented in Table 19.

Table 19 - Volumetric Analyses Results

	Actual - Numerical Simulation	Geostatistics - 165 well logs	Geostatistics - 48 well logs
IOIP, MRbbl	7,605,000.00	8,151,984.00	8,639,531.00
Error (%)		7.19	13.60

4.2. Synthetic Model Application

At the beginning the results of each model's training and verification is presented and discussed. Then the production prediction from the Time Successive Model is demonstrated and compared to the real data from the simulation results.

4.2.1. Initial Production Rate Model

This model which is the most uncertain part of the prediction is predicting the initial rate of the new wells. Previously we discussed that this neural network model is trained based on existing well instances during the reservoir's lifetime.

The training set contains 133 well records. The cross plot for predicted initial rate values and the actual value of the flow rate is shown in Figure 19.

Figure 19 - Initial Rate Model, Training Set Cross Plot

The same cross plot is generated for calibration and verification datasets.

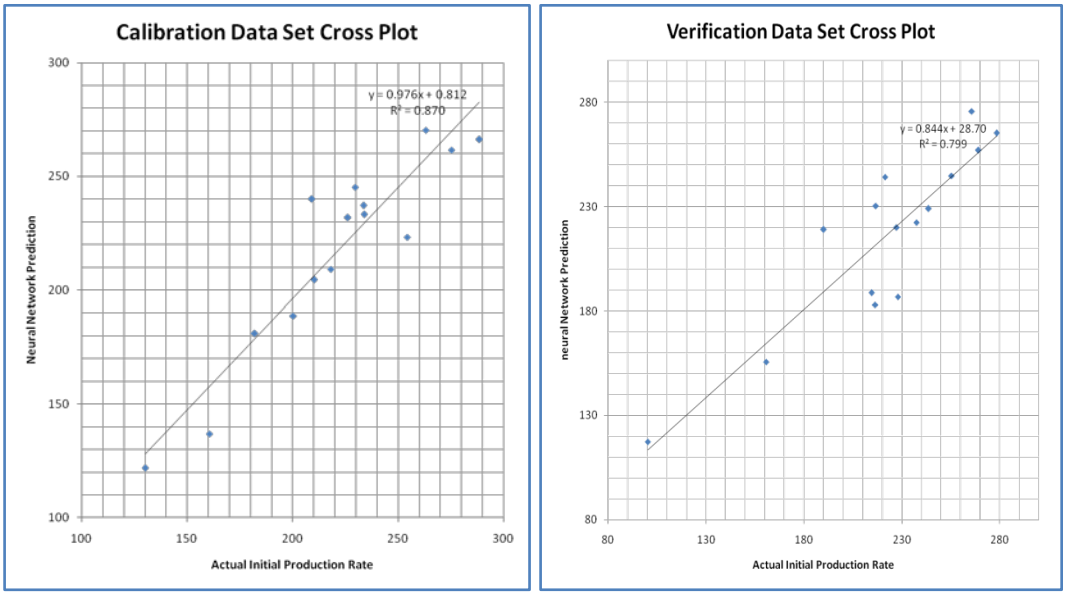

Figure 20- Initial Rate Mode -Calibration Set Cross Plot (Left) - Verification Set Cross Plot (Right)

This model's percentage error is calculated by comparing the predicted results with actual values from numerical simulator. An error frequency and cumulative distribution is shown in Figure 21.

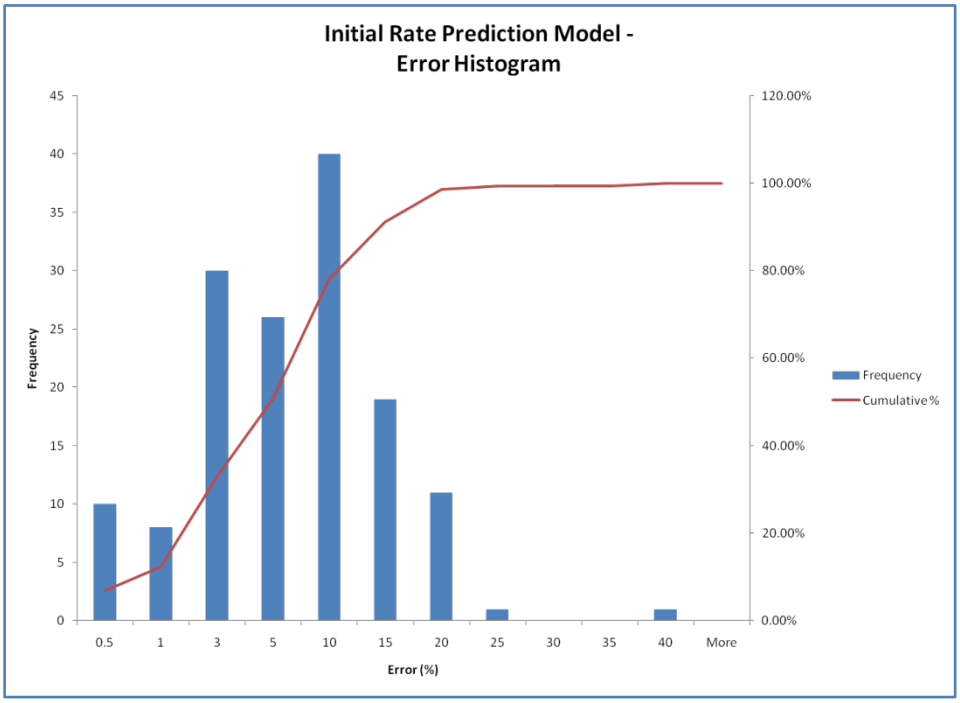

Figure 21 - Initial Rate Model - Error Distribution

4.2.2. Second Month Production Rate Model

After predicting the Initial rate, the second month production is modeled by a neural network which is trained in the same manner. In this model again we use 153 data instances which are available. 10 % of the data is used for calibration and another 10% is kept for verification of the model.

Results of training the network is shown in Figure 22 - Second Month Rate Model, Training Set Cross Plot. As it can be observed the uncertainty of the prediction have decreased a lot since more information about the wells is available when predicting the second month production.

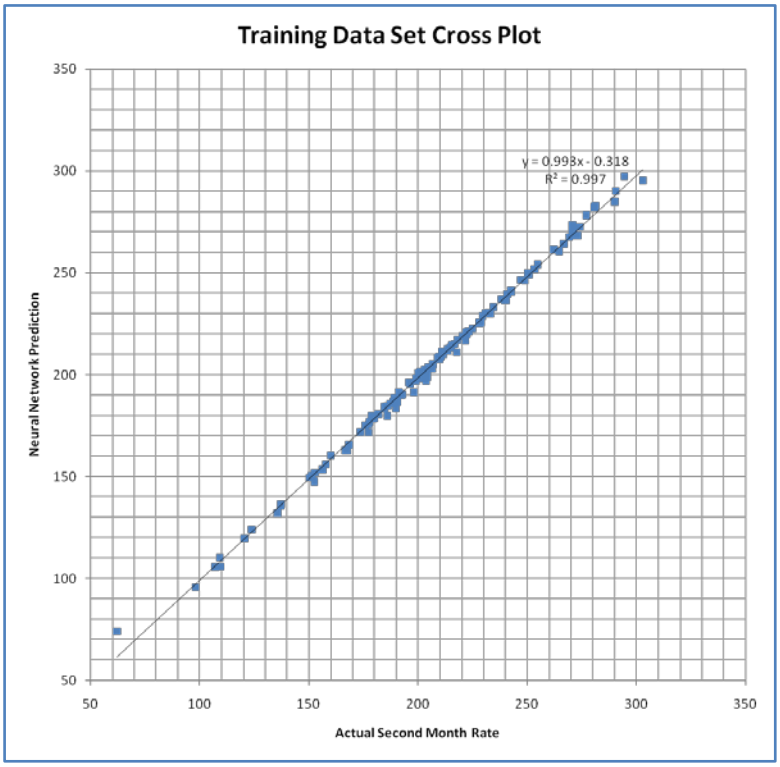

Figure 22 - Second Month Rate Model, Training Set Cross Plot

The calibration and verification data sets also show a promising accuracy in the prediction.

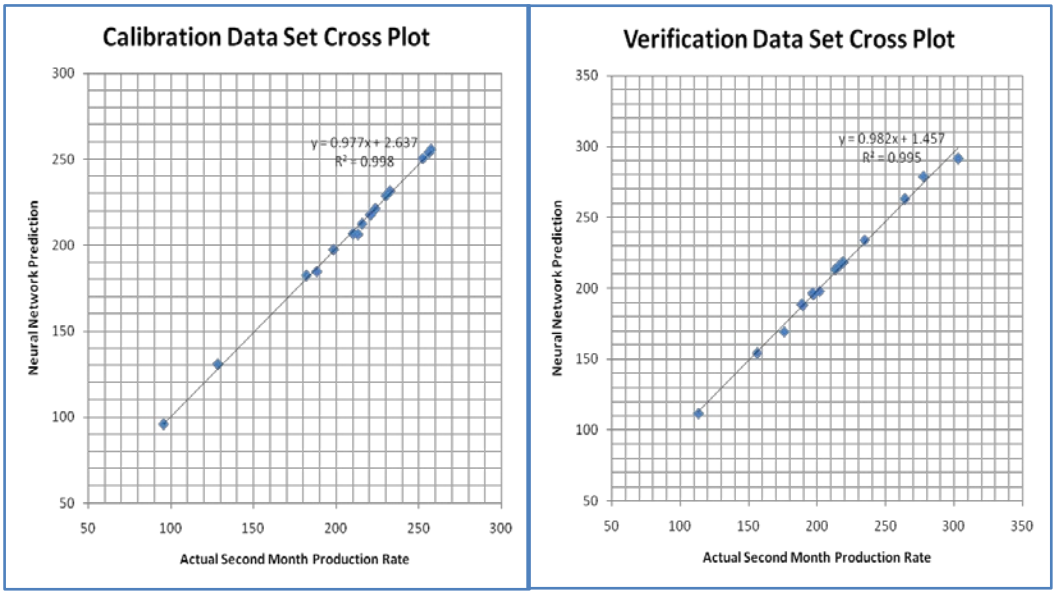

Figure 23 - Second Month Rate Mode -Calibration Set Cross Plot (Left) - Verification Set Cross Plot (Right)

An error distribution is also generated for this model.

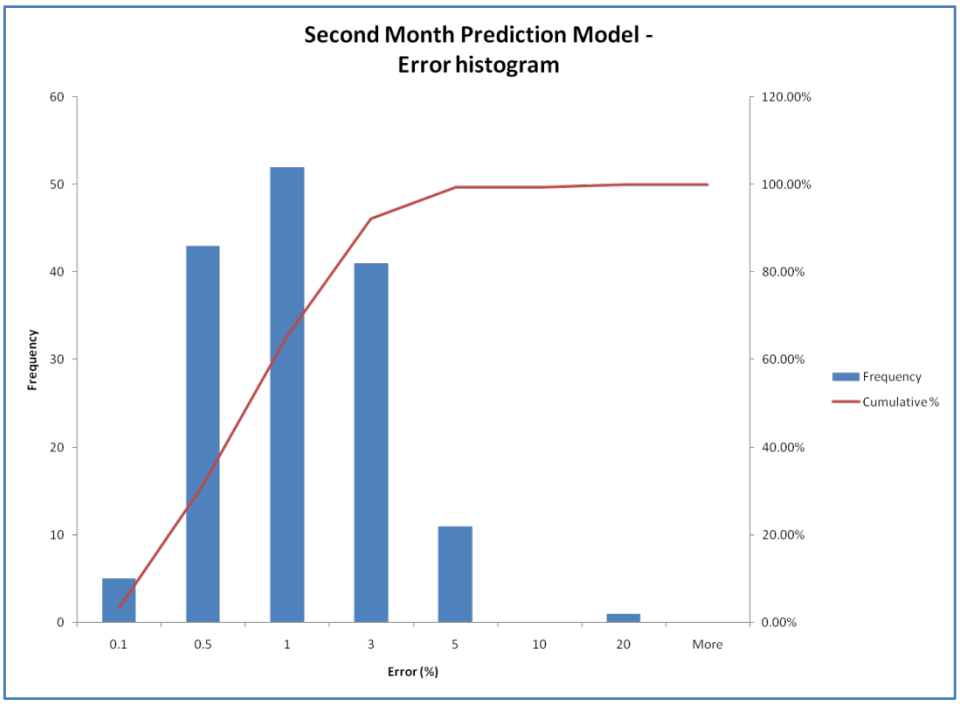

4.2.3. Third Month Production Rate Model

The last model which predicts the production rate at a specific well age is the third month production prediction model. This model has 150 data inputs and slightly different from the previous two models uses a 90%, 5%, 5% segmentation for training, calibration and verification.

Results of training the network is shown in Figure 24

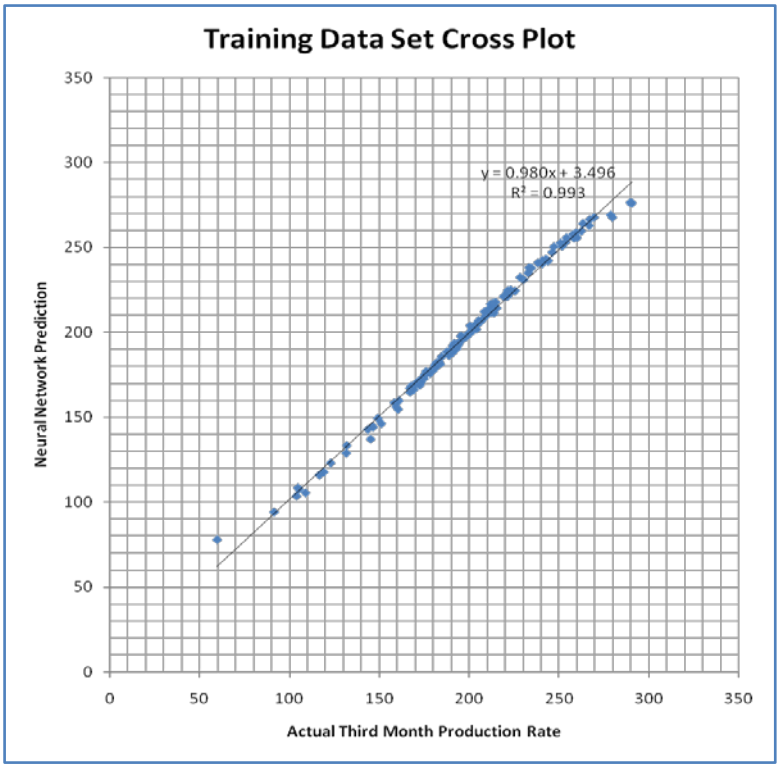

Figure 24 - Third Month Rate Model, Training Set Cross Plot

And also the calibration and verification sets cross plots is shown in Figure 25.

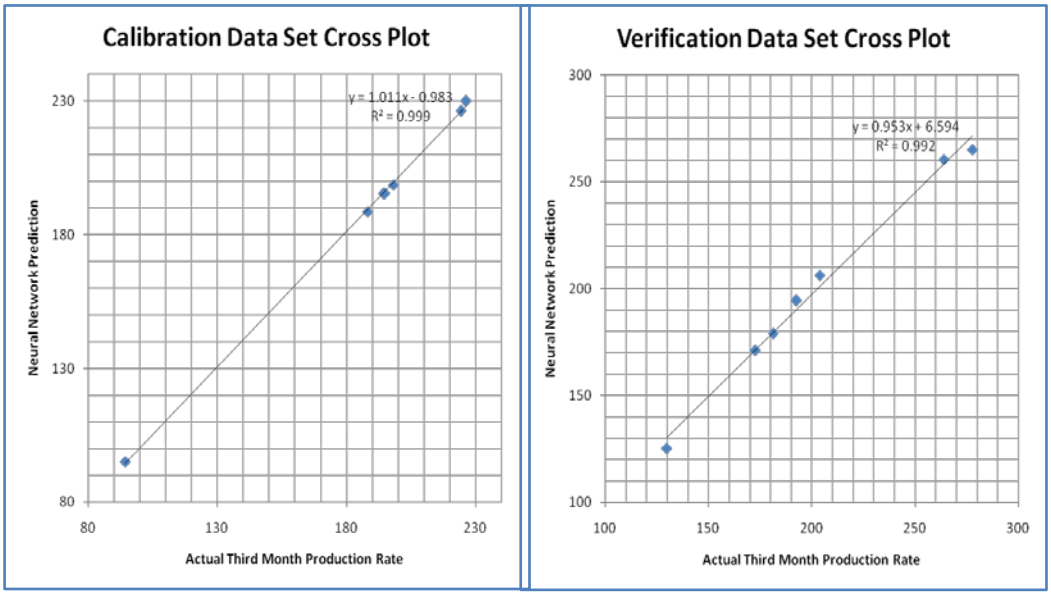

Figure 25 - Third Month Rate Mode -Calibration Set Cross Plot (Left) - Verification Set Cross Plot (Right)

And as usual to measure the precision of the network's prediction an error distribution is shown in Figure 26.

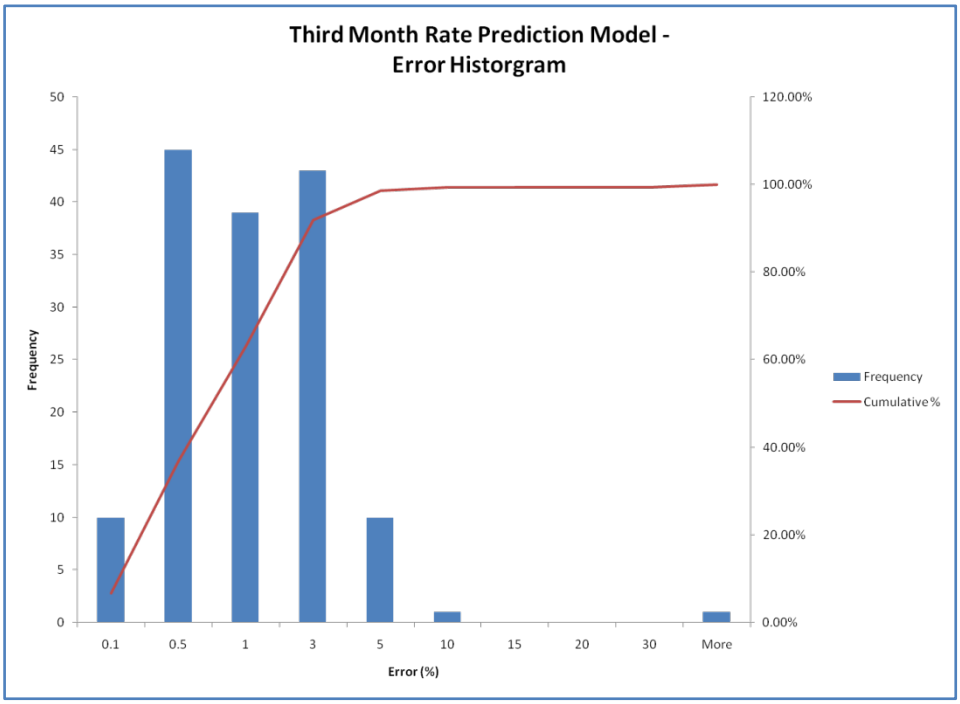

Figure 26 - Third Month Model Error Distribution

4.2.4. Production Tail Model

In this part results for the production tail model is discussed. This model is supposed to be predict the production rate change at each time of well's life time after the third month of production. The model is trained, calibrated and verified with about 5700 data records. Data is partitioned with a 60% training fraction, 20% calibration and 20% verification part.

Training Dataset cross plot is shown in Figure 27. The rate change is predicted with an R^2=0.903. This implies a rate prediction of very high accuracy in the time successive model.

Clarification and Verification data set is also shown below. These graphs show that the trained network works very well for the blind data as well.

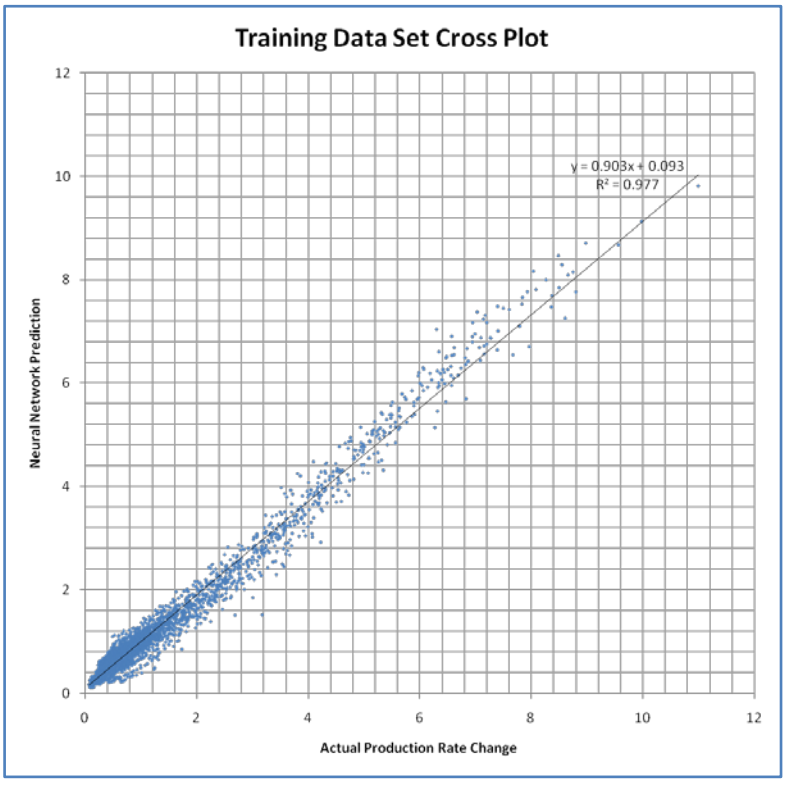

Figure 27 - Production Tail Model Training Set

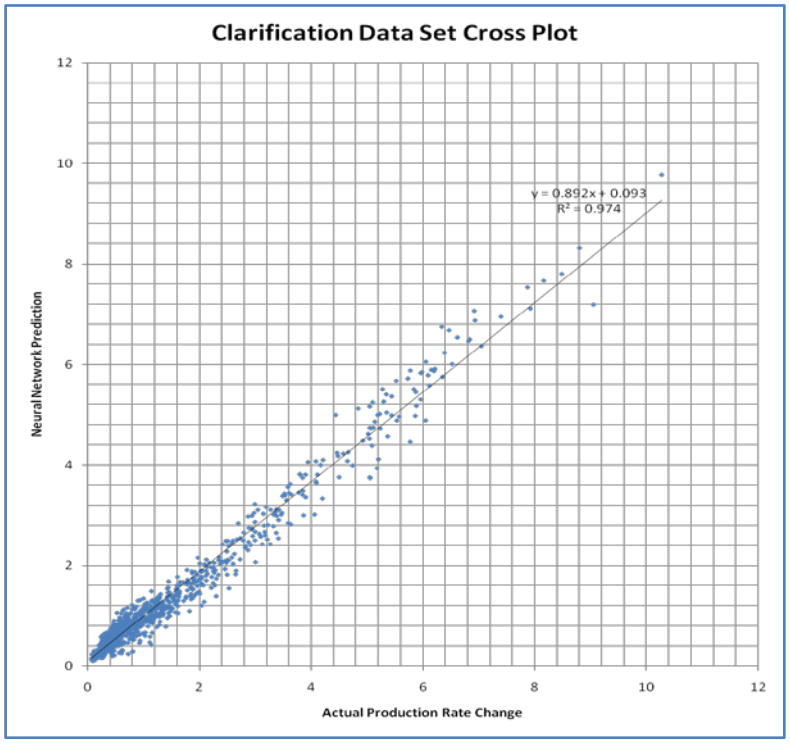

Figure 28 - Production Tail Model Calibration Set

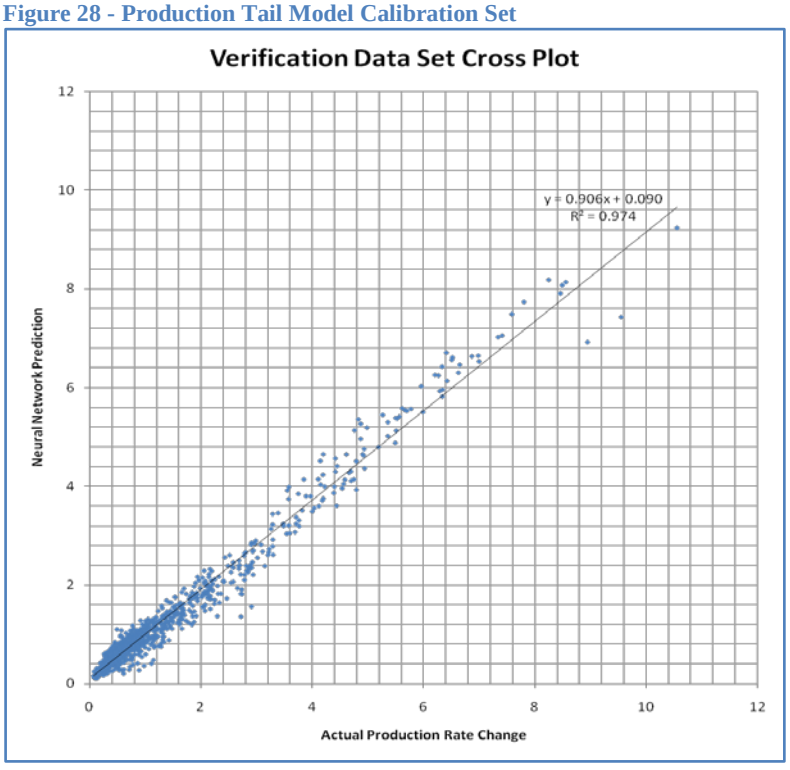

Figure 29 - Production Tail Model Verification Set

Because of very small values of the output parameter the absolute value of the error is shown in Figure 30. In this case absolute value shows a better understanding of model's prediction capabilities rather than the percentage error.

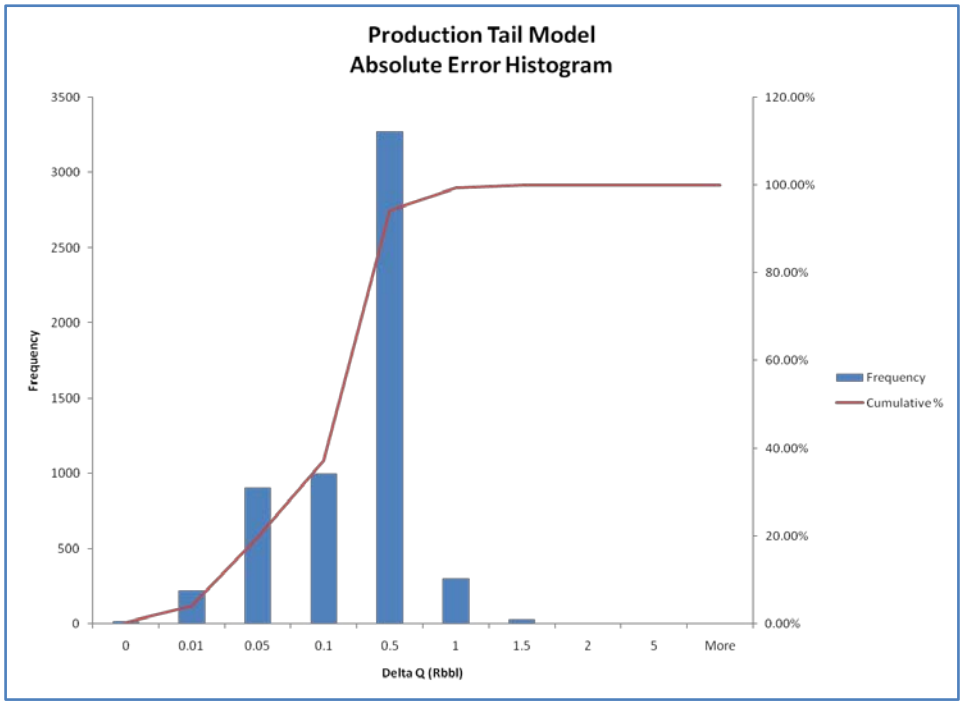

Figure 30 - Tail Model, Delta Q Prediction - Absolute Error Distribution

4.2.5. Time Successive Model

Once all the neural networks showed a satisfying predictive capability they were integrated in the time successive model. Production data were recorded from the simulation model from beginning of 1982 which was the first date of production of the first set of wells. Five years of this production data was used for training purposes and another year was kept for verification.

Time successive predictive model was initiated on 1/1/1987. A one year prediction of all the wells, Including 9 wells that were drilled after this date is compared to the real production data from numerical simulator results.

New wells' production prediction is the main objective of this work. The entire fields and all existing wells production is also predicted and can be compared to the conventional decline curve analysis results. The precision of these predictions will increase the validity of new wells' production prediction. This let us to actually predict the decline behavior of a well which hasn't been drilled yet. This will lead to better decision makings and performance assessments.

Nine wells were kept out of all the trained models and now their production is estimated through the time successive prediction model. These flow predictions are compared with real results taken from numerical simulator. Figure 31 through Figure 39 are showing the nine new wells' flow rate profile and cumulative production comparison. In these Figures the actual production rate is shown in red and the production prediction is in blue. The purple curve shows the actual cumulative production while the green curve is showing the predicted cumulative production.

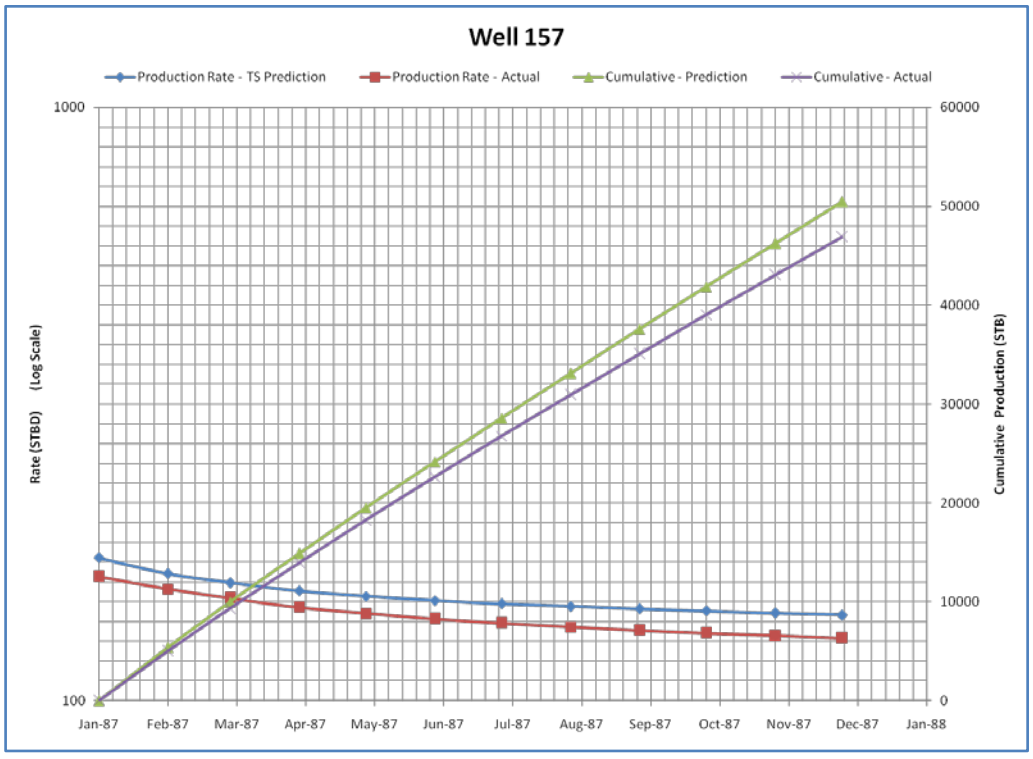

Figure 31 - Well 157 Production Rate and Cumulative Comparison

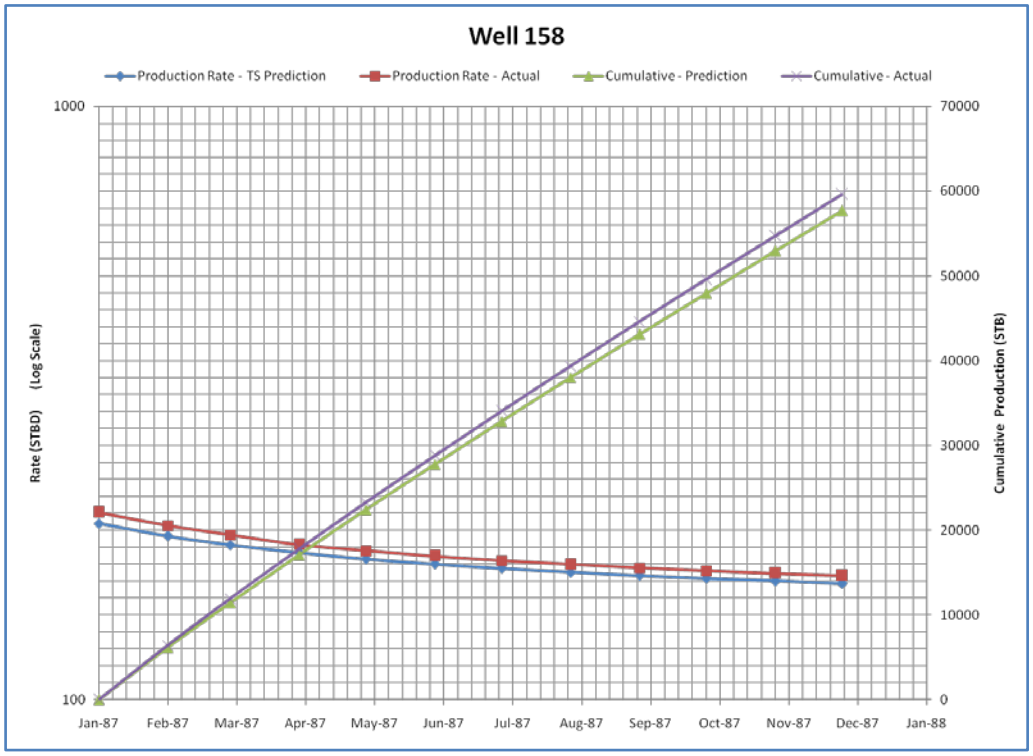

Figure 32 - Well 158 Production Rate and Cumulative Comparison

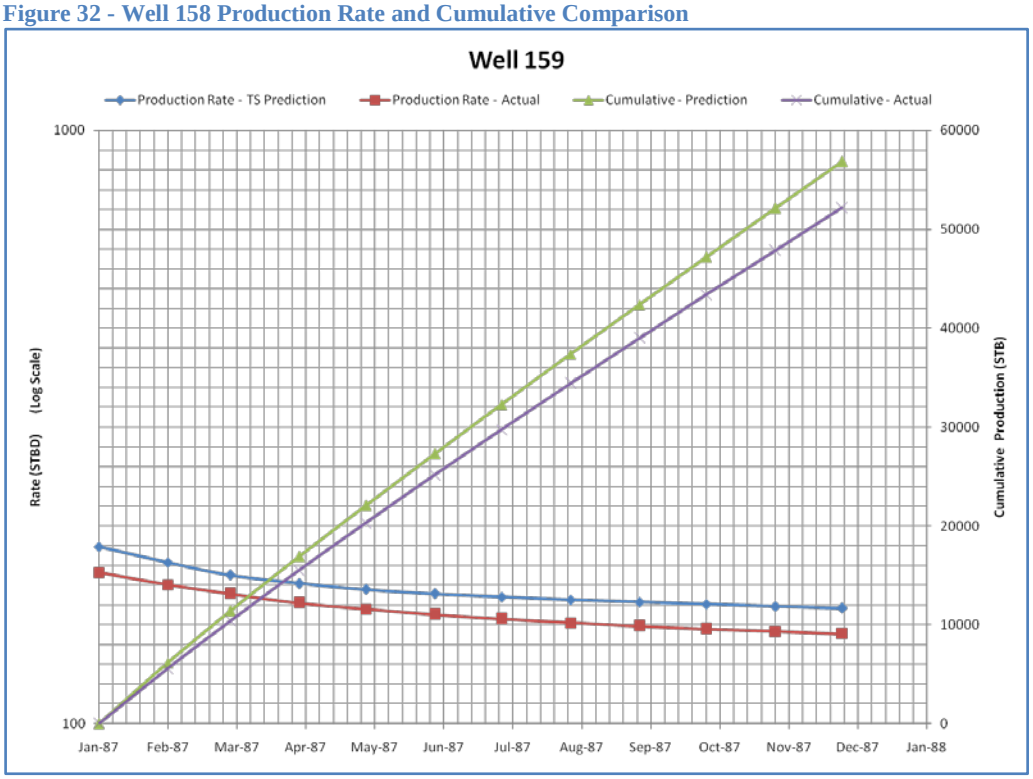

Figure 33 - Well 159 Production Rate and Cumulative Comparison

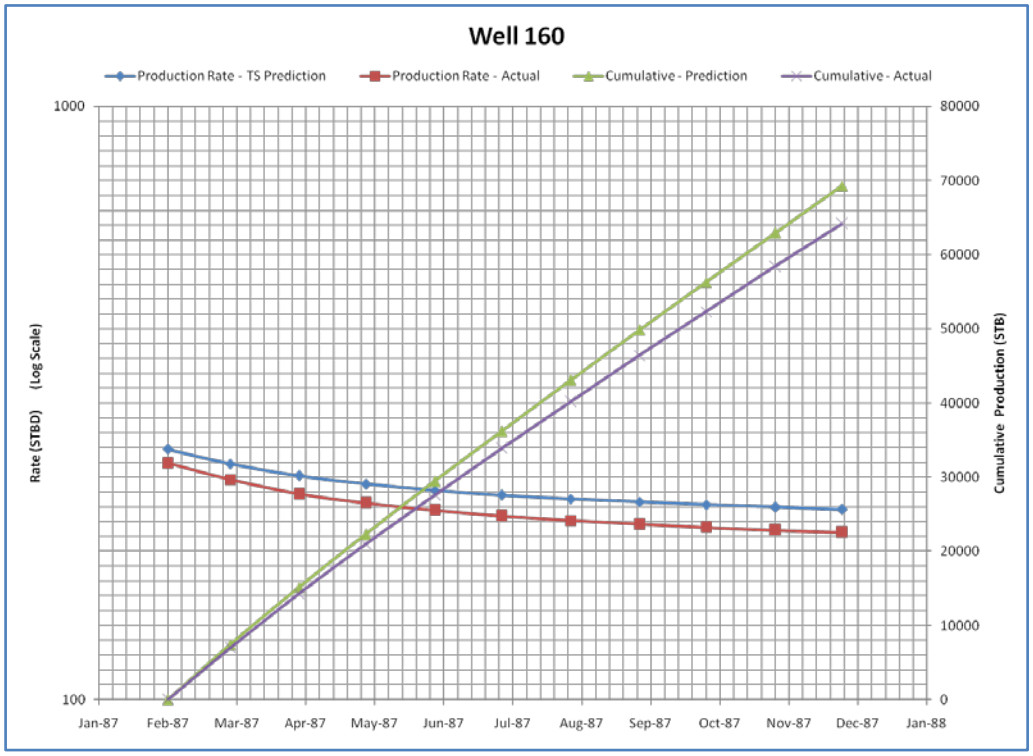

Figure 34 - Well 160 Production Rate and Cumulative Comparison

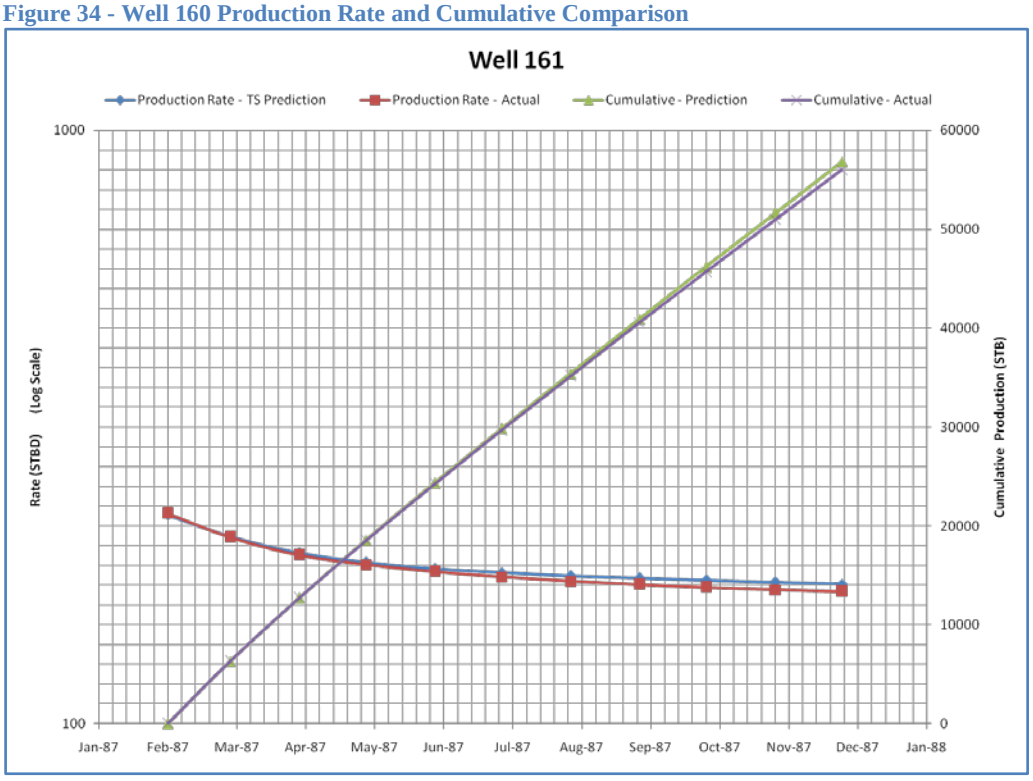

Figure 35 - Well 161 Production Rate and Cumulative Comparison

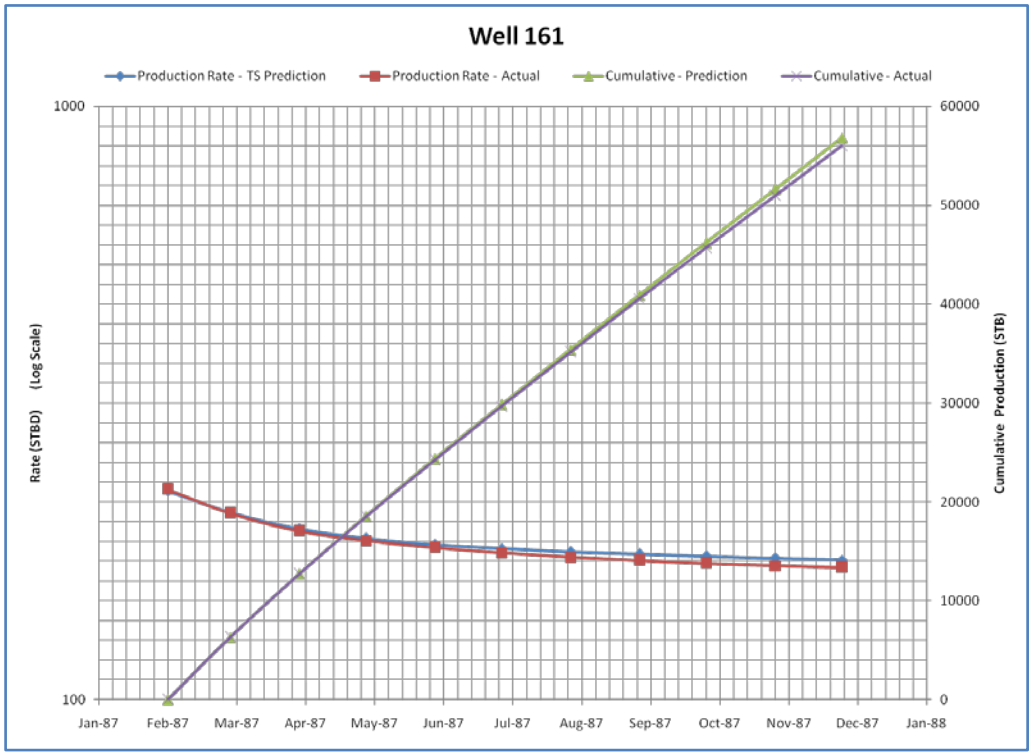

Figure 36- Well 162 Production Rate and Cumulative Comparison

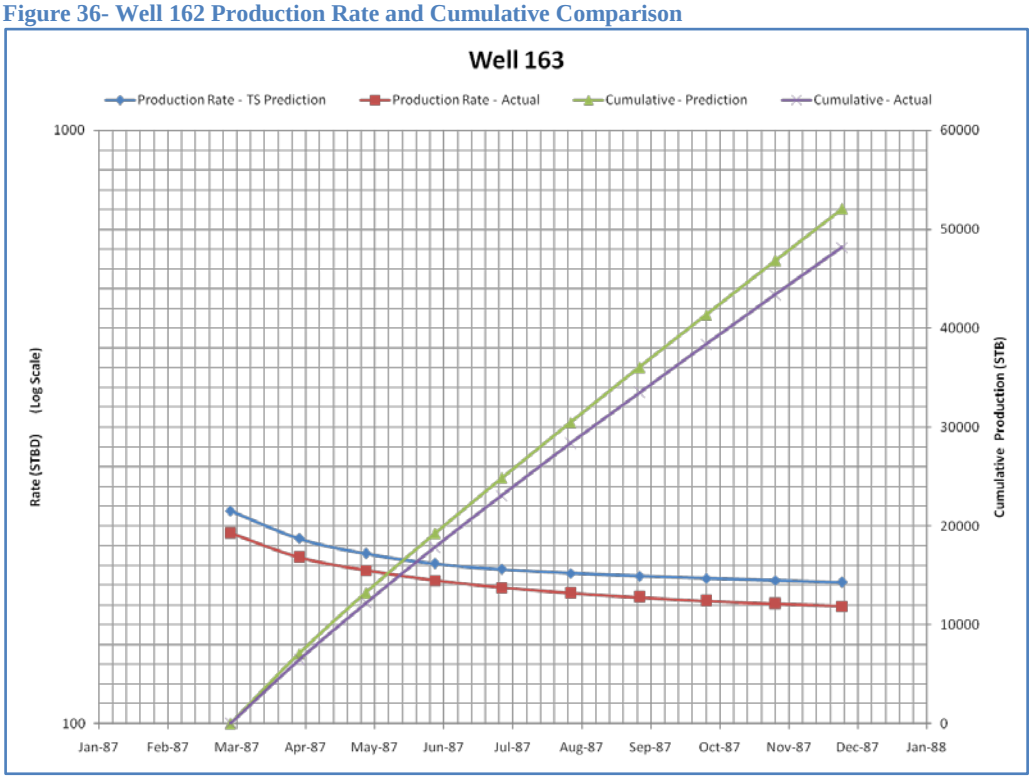

Figure 37 - Well 163 Production Rate and Cumulative Comparison

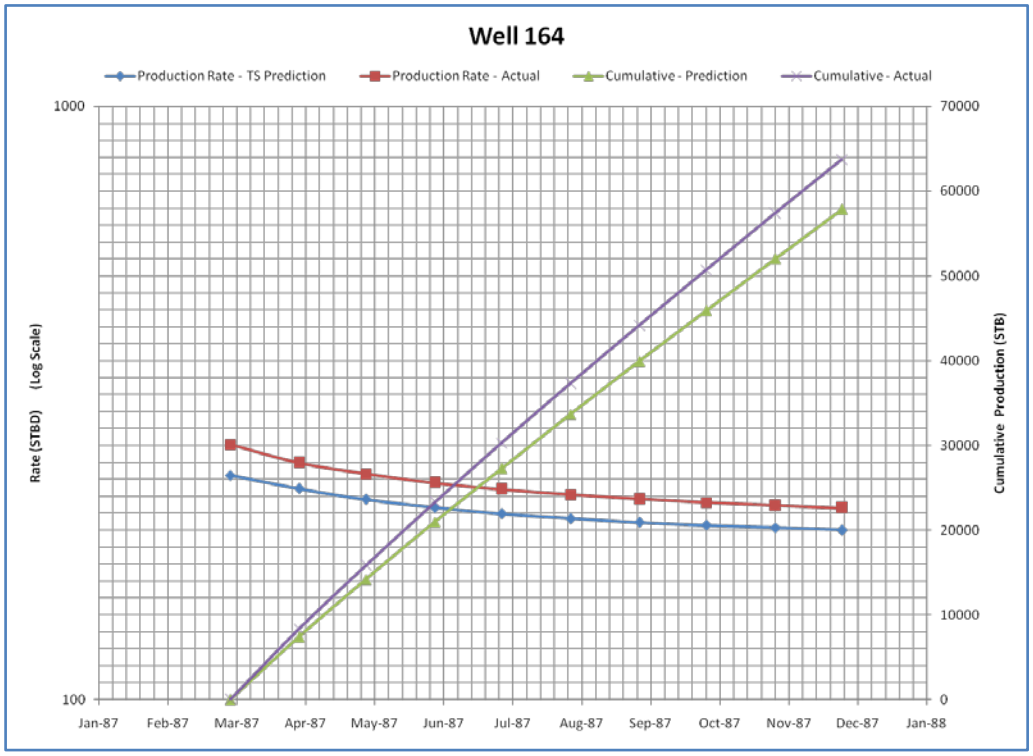

Figure 38 - Well 164 Production Rate and Cumulative Comparison

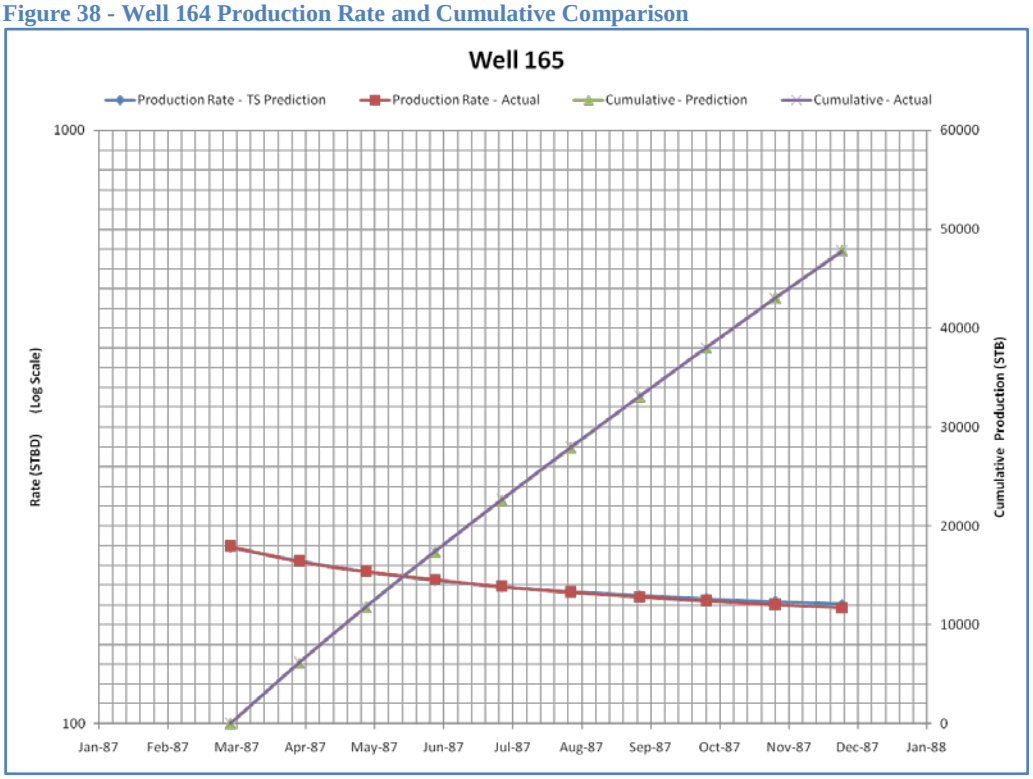

Figure 39 - Well 165 Production Rate and Cumulative Comparison

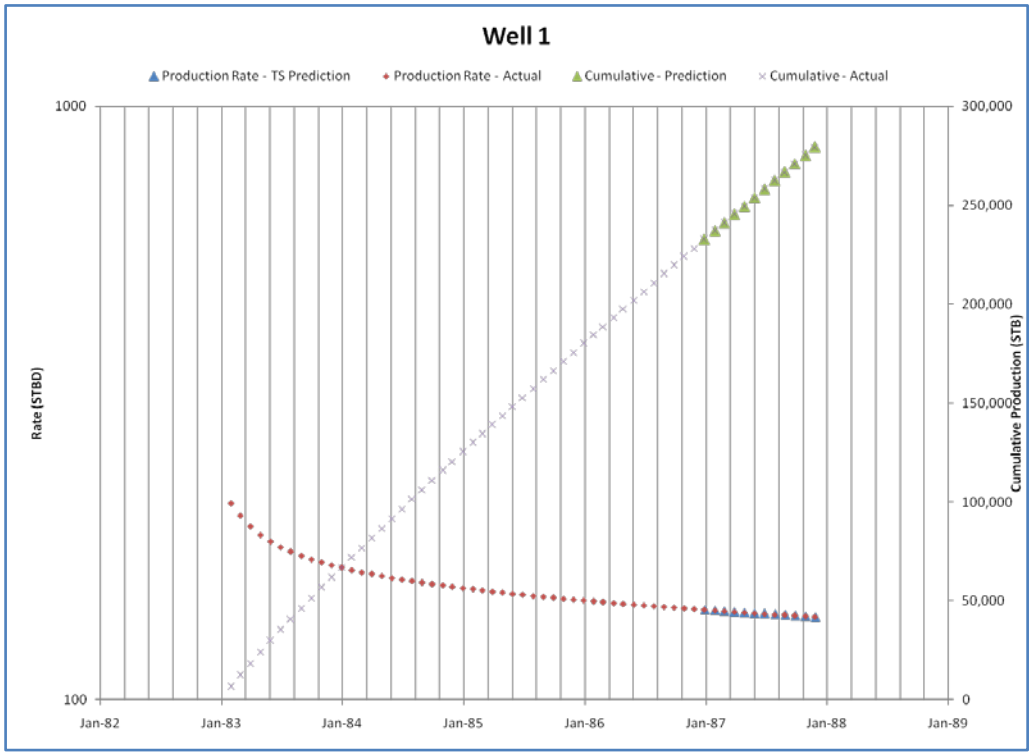

Figure 40 - Well 1 Production Rate and Cumulative Comparison

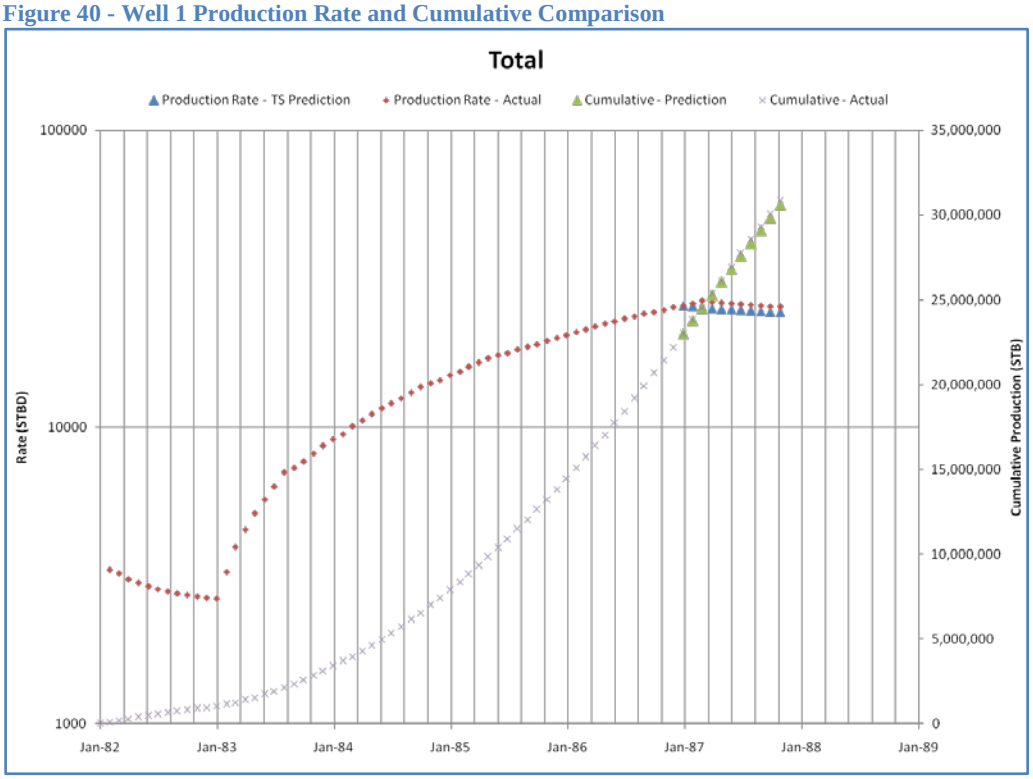

Figure 41 - Total Field Production Rate and Cumulative Comparison

Production rate and cumulative prediction for one of the oldest wells and for the entire field is shown in Figure 40 and Figure 41. The total field production prediction shows that the ITSPM is performing consistently on all the wells in different location with different ages.

The error distribution for production rate prediction and cumulative production is presented in Figure 42 and Figure 43. As it is clear in both distributions more than 50% of the instances have less than 1% error. Although a maximum error of 11.23% in production rate and 12.65% in Cumulative production is observable.

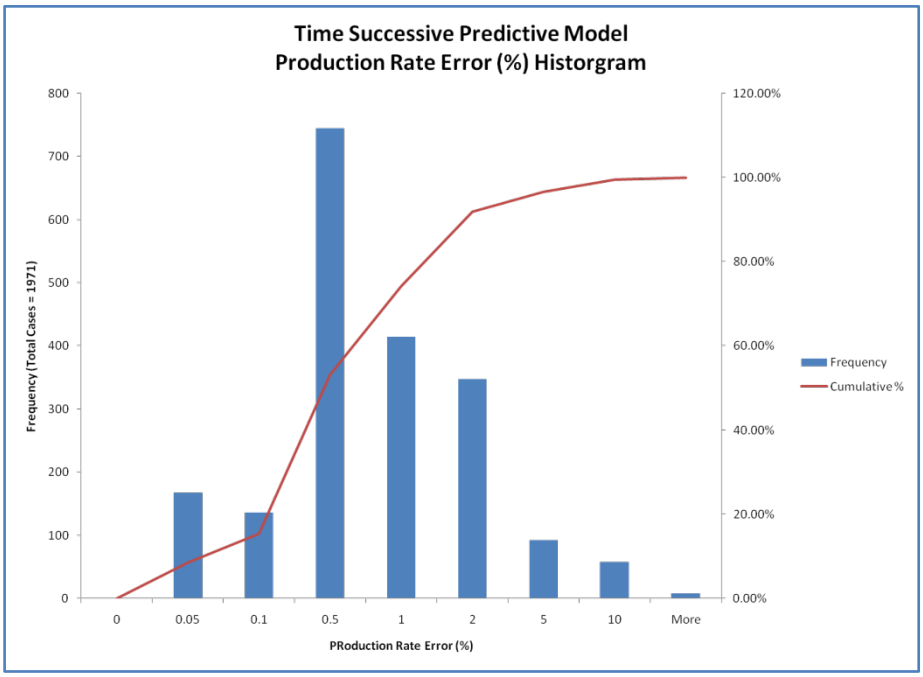

Figure 42 - Production Rate Prediction Error Distribution

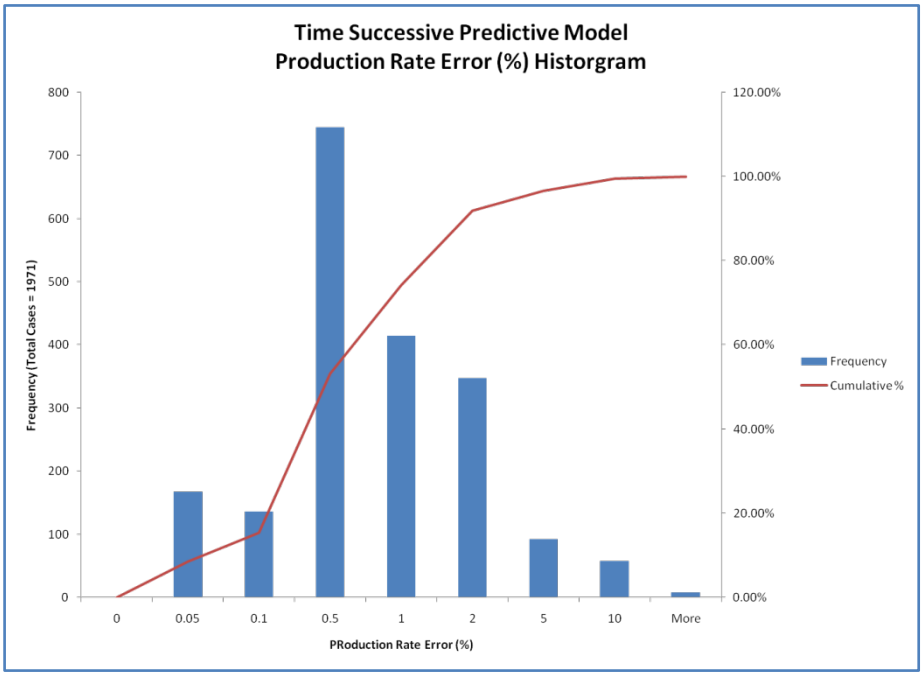

Figure 43 - Cumulative Production Prediction Error Distribution

4.3. Sensitivity Analysis

As we all know all pieces of information we have about any reservoir characteristics are subject to a high degree of uncertainty. Well log information is normally available for a few percent of existing wells in the field. Moreover they are not an exact representation of geological characteristics and have an amount of uncertainty associated to them.

Also the modeling part will have some uncertainty into it due to the errors associated with any predictive model. Therefore the predicted values for production rate will not be exact.

In order to account for all these uncertainties and have a sense of their effect on our technique, a triangular distribution is considered for all the input values with a support range equal to 40% of the total range for that parameter and the actual value is the most likely value of the distribution.

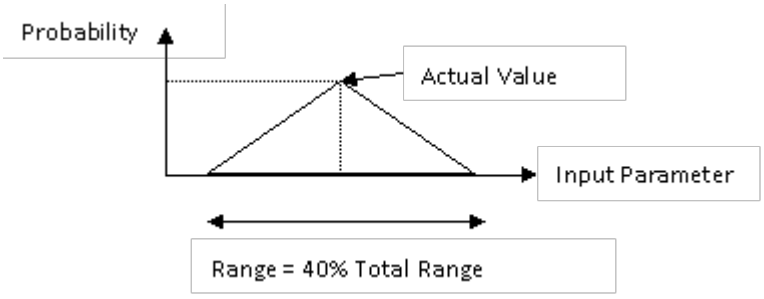

Figure 44 - Triangular Distribution for Model Input Parameters

A montecarlo simulation is performed for each predictive model using these input value distributions. Model's output would also be represented with a triangular distribution which we can extract a most likely decline of production and a maximum and minimum range from that.

Results of this montecarlo simulation are presented for three of new wells. These results can be compared to the ones from section 4.2.5.

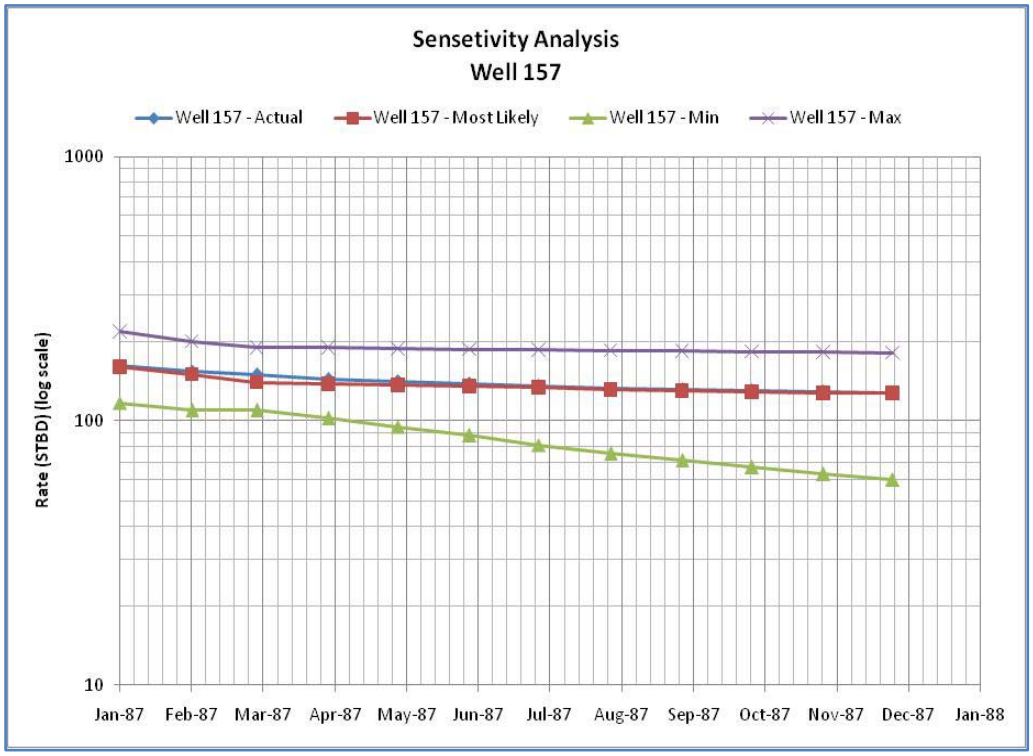

Figure 45 - Well 157 Sensitivity Analyses

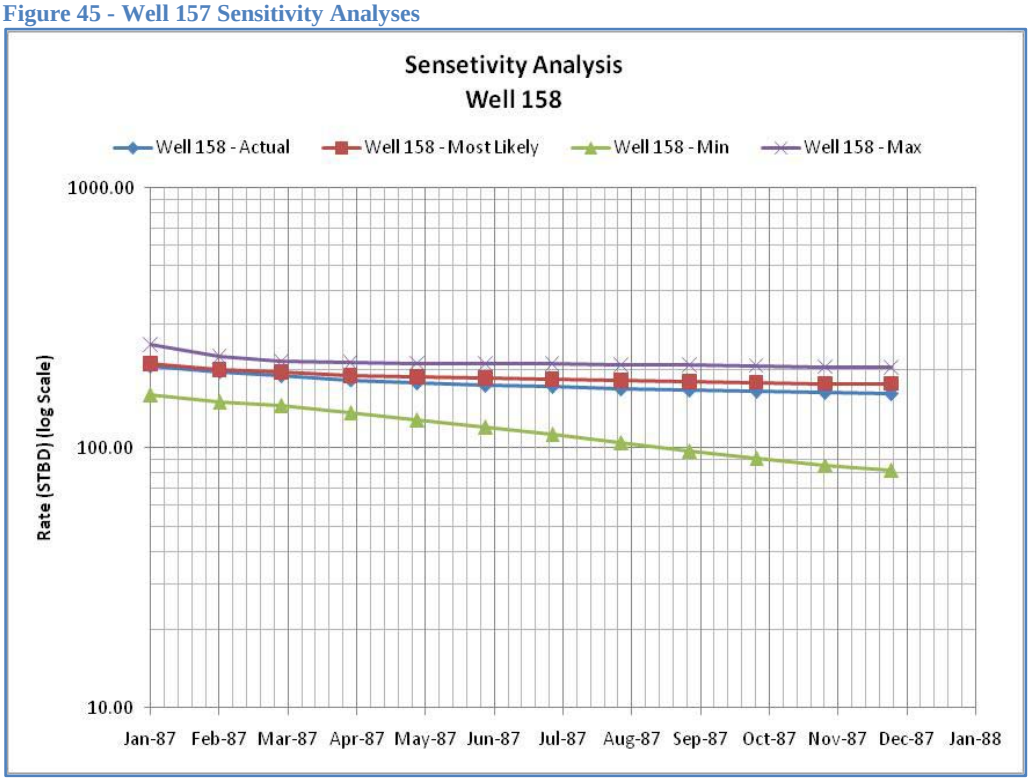

Figure 46 - Well 158 Sensitivity Analyses

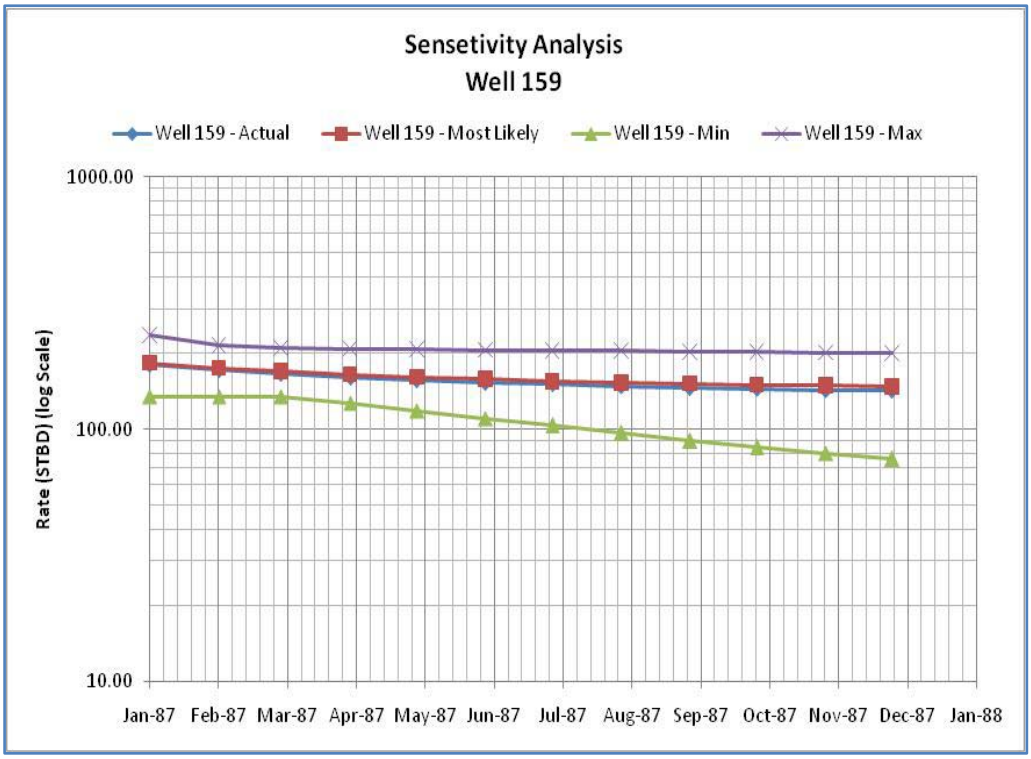

Figure 47 - Well 159 Sensitivity Analyses

As it can be seen in the figures the most likely prediction stays very close to the real production profile despite the uncertainties involved with all the input parameters while the minimum and maximum range are showing the extent of possible output values from this technique.

4.4. Real Reservoir Application

Four different neural networks are trained for Time Successive Prediction. First and most uncertain model is the initial rate prediction model. In this model 97 well records are used in the dataset. 10% of the data is used for calibration and 10% are kept out for verification of the network. This networks prediction performance cross plot is shown in Figure 48.

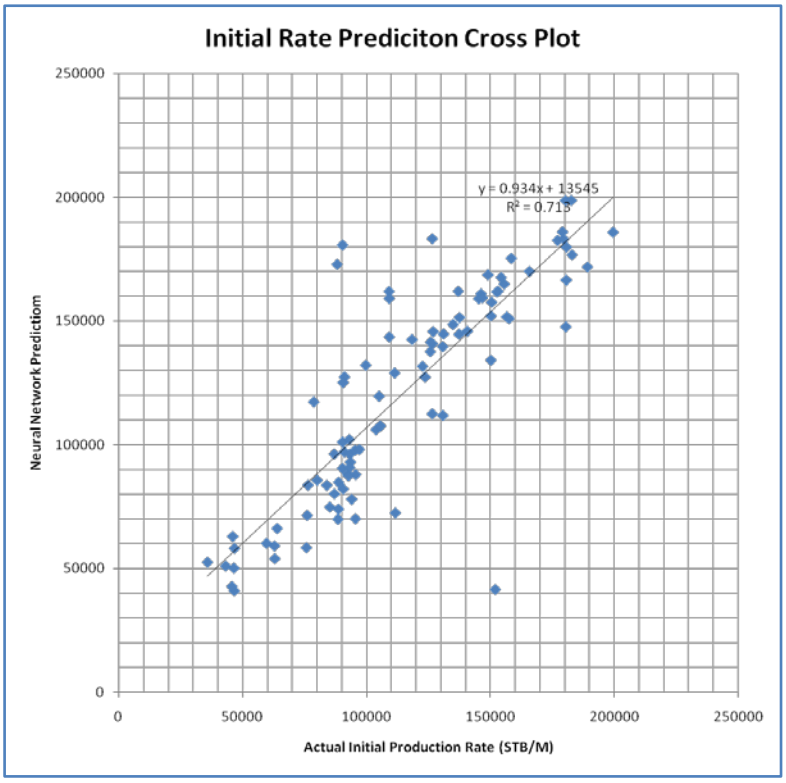

Figure 48- Initial Rate Prediction Model - Cross Plot

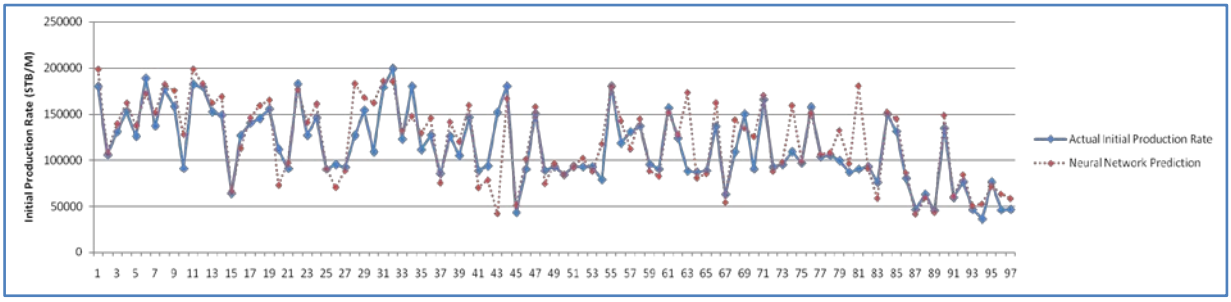

Figure 49 - Initial Production Prediction Model - Performance Behavior

A distribution of the initial rate prediction error (%) is shown in Figure 50. This figure shows more than 80% of the predictions are experiencing less than 30% error.

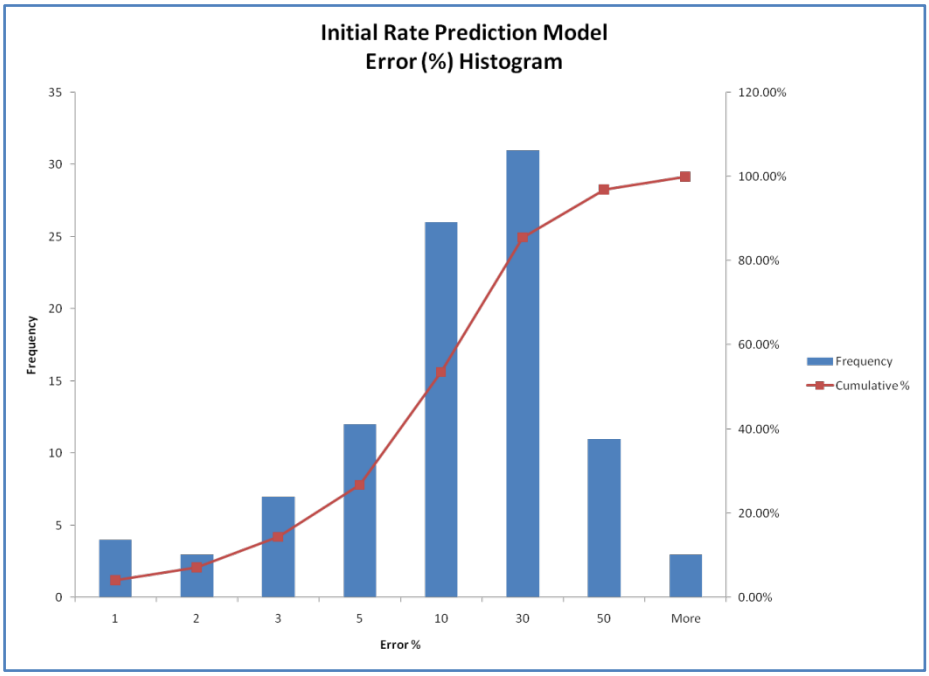

Figure 50 - Initial Rate Prediction Model - Error (%) Distribution

Second Month Cumulative Production model also uses 85 most recent well records. This data set is used to train, calibrate and verify the network to predict the second month cumulative production. 10% of the data is used for calibration and 5% are used for verification. A cross plot of this networks performance is shown in Figure 51.

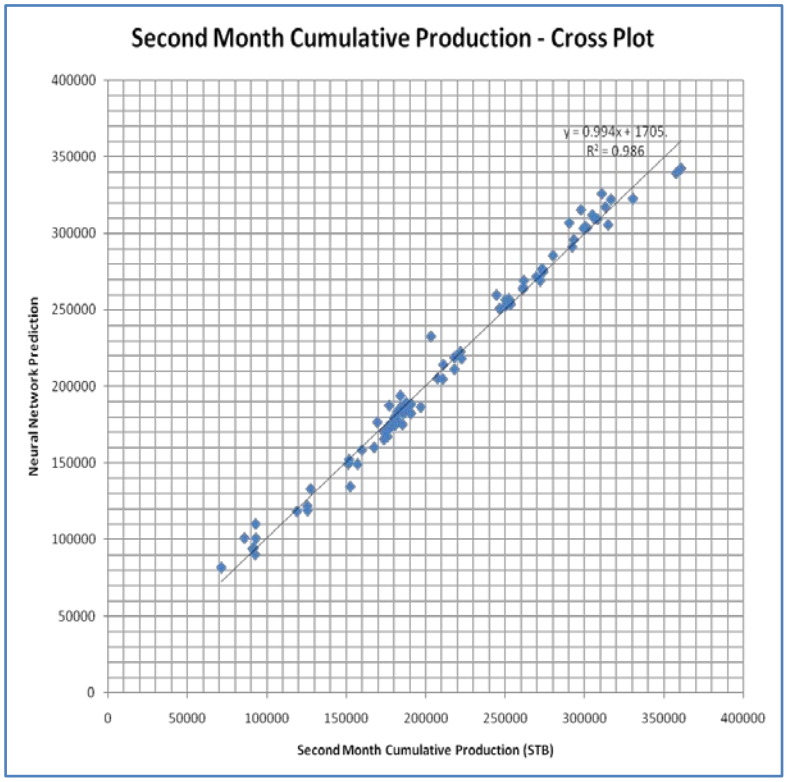

Figure 51 - Second Month Cumulative Prediction Model - Cross plot

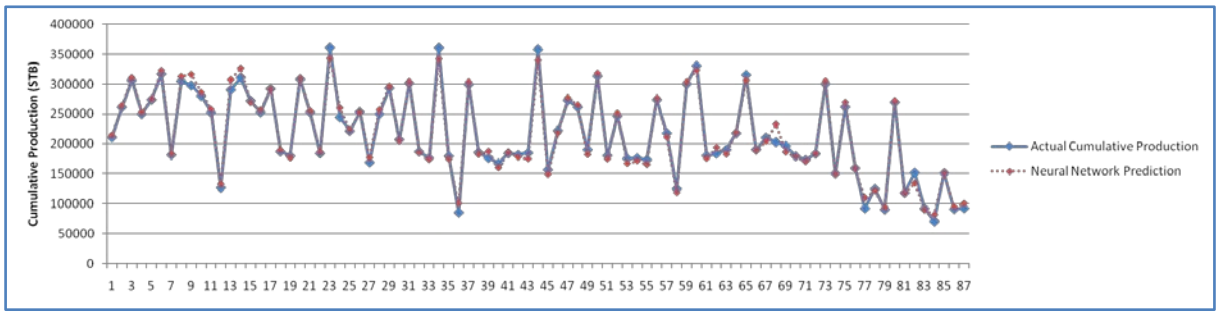

Figure 52 - Second Month Cumulative Prediction Model - Performance Behavior

In order to show the performance of the model, an error distribution is presented as well. As it is apparent in this figure, about 80% of the predictions have less than 5% error.

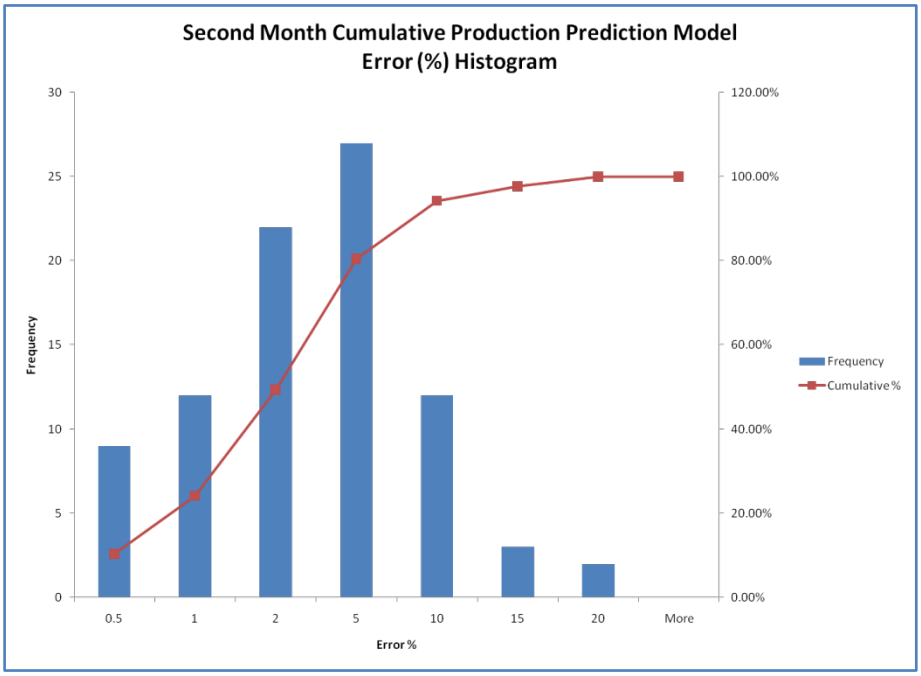

Figure 53 - Second Month Cumulative Prediction Model - Error (%) Distribution

Next model is designed to predict the cumulative production in third month. Dataset has 104 data records that 85% is used for training, 10% is used for calibration and 5% for verification of the model. Performance of this model is demonstrated in a cross plot in Figure 54. Also the error distribution of this model is shown in Figure 56.

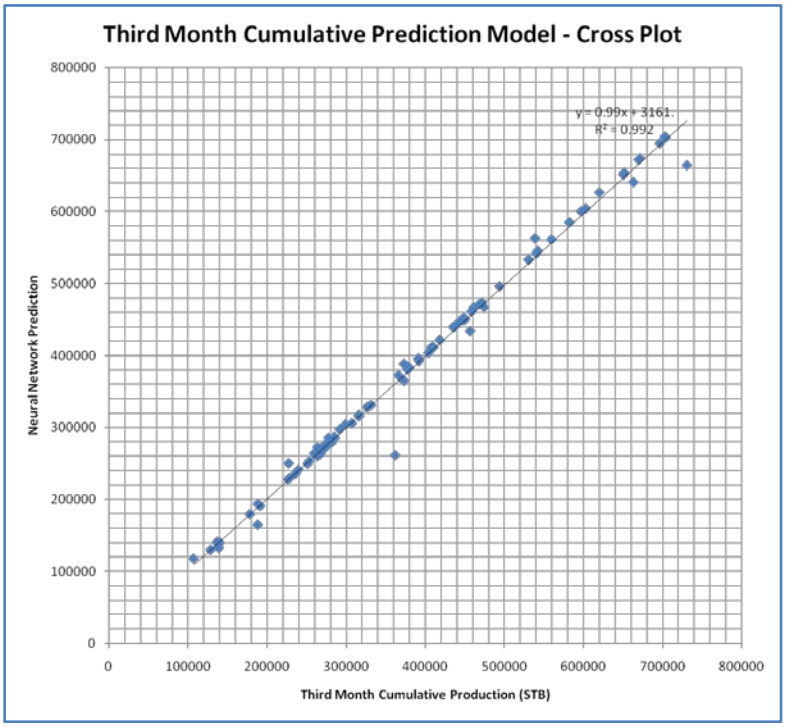

Figure 54 - Third Month Cumulative Prediction - Cross Plot

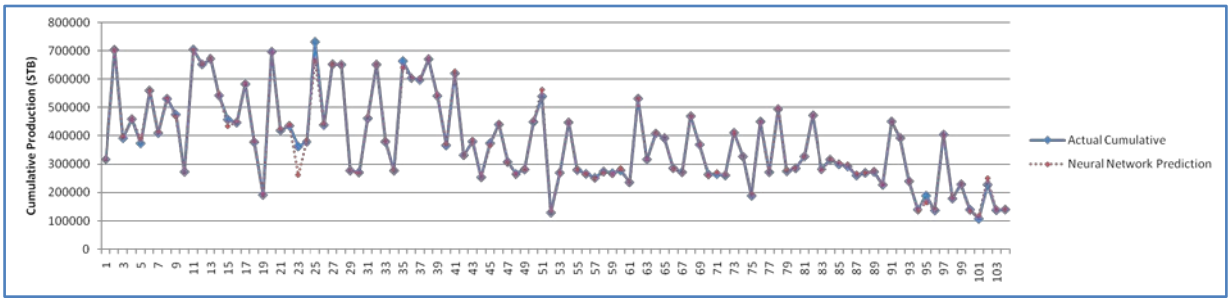

Figure 55 - Third Month Cumulative Prediction Model - Performance Behavior

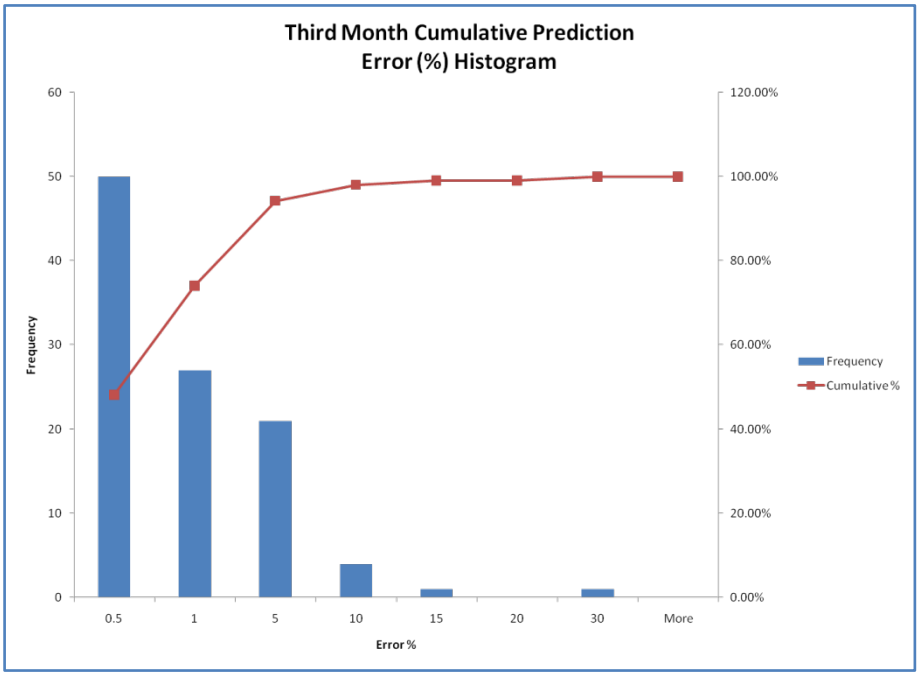

Figure 56 - Third Month Cumulative Model -Error Distribution

Last model that is trained to predict the rest of the cumulative production profile uses 85 data records with 90% training, 5% calibration and 5% verification set up. This model uses three preceding cumulative productions to predict the next step's value. Performance of this model is demonstrated in Figure 57 and Figure 58. Error distribution of this model is also provided.

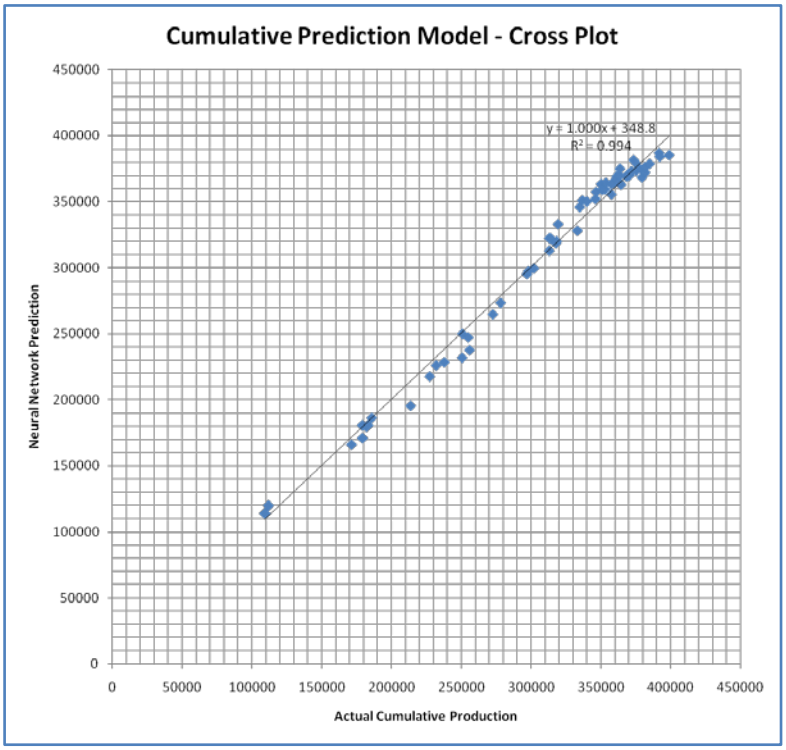

Figure 57 - Cumulative Model Prediction - Cross Plot

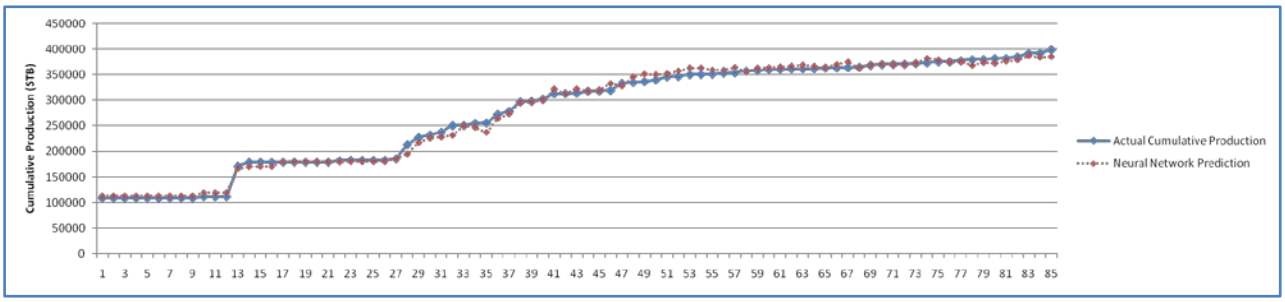

Figure 58 - Cumulative Prediction Model - Performance Behavior

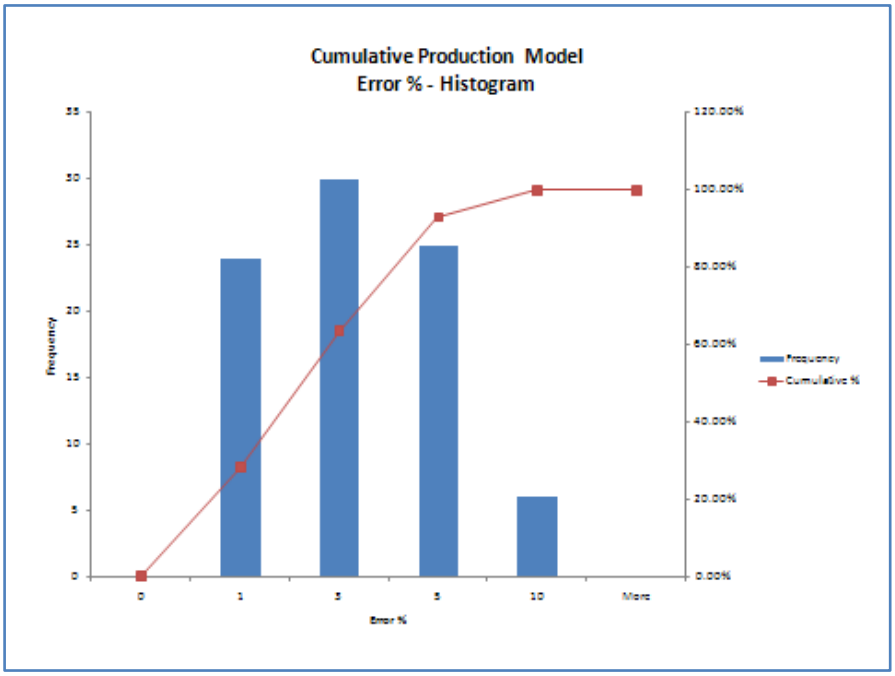

Figure 59 - Cumulative Model -Error Distribution

4.4.1. Time Successive Production Prediction

Now that all the models are trained and verified, they can be used to predict the future production of 4 new wells. These wells as described before have not been used in any of the datasets and none of their characteristics haven't been available to the networks. These four wells location are shown in Figure 60.

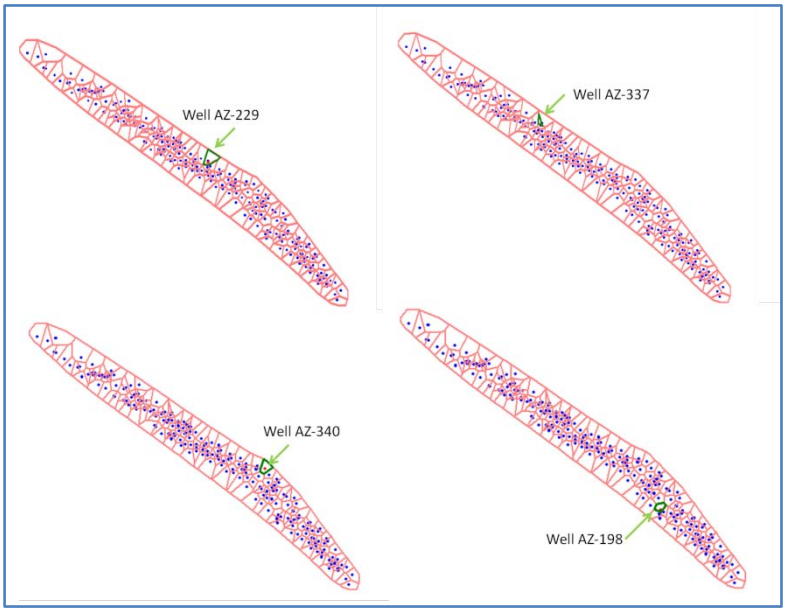

Figure 60 - Four Verification Well Location

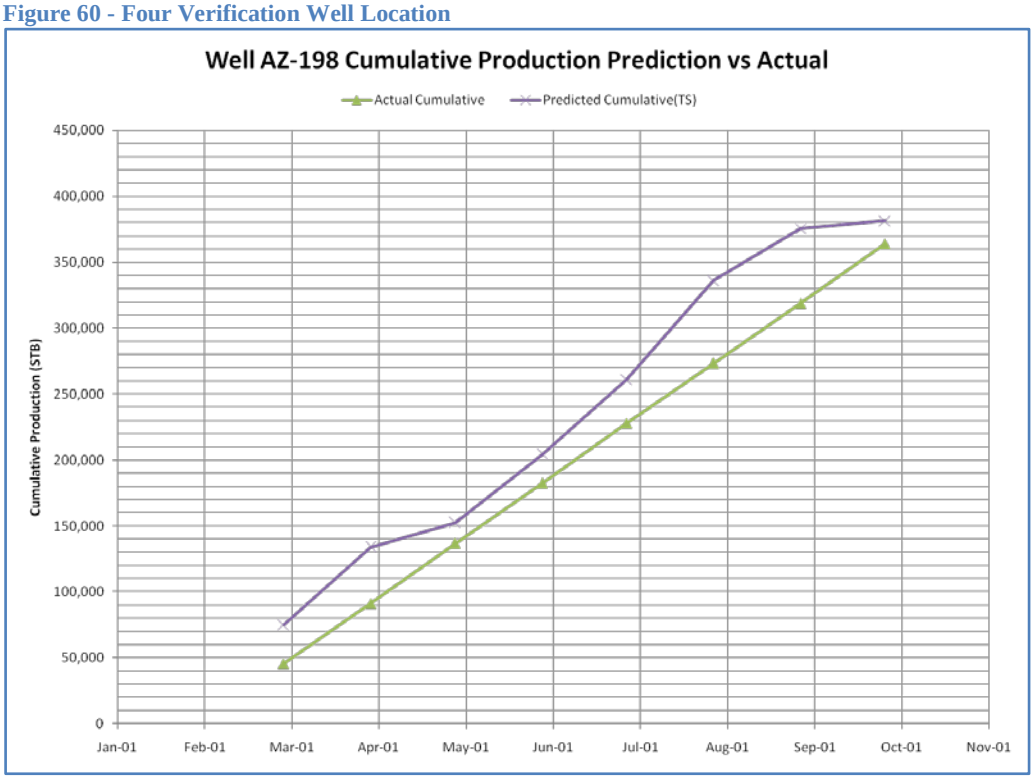

Figure 61 - Well AZ-198 Cumulative Profile Comparison

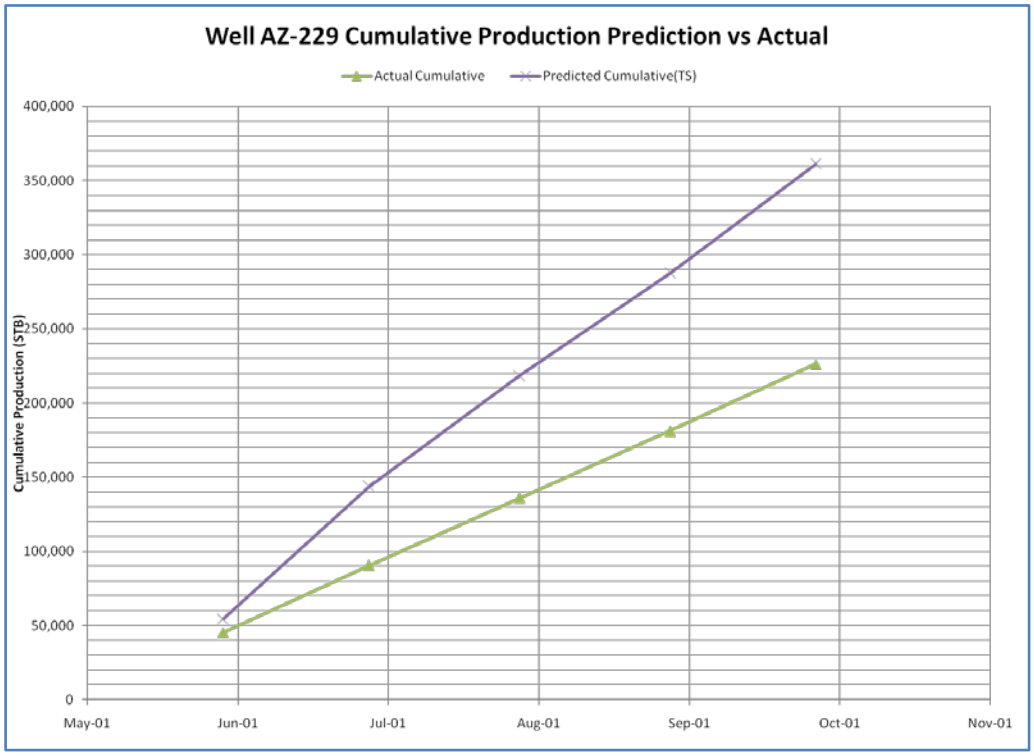

Figure 62 - Well AZ-229 Cumulative Profile Comparison

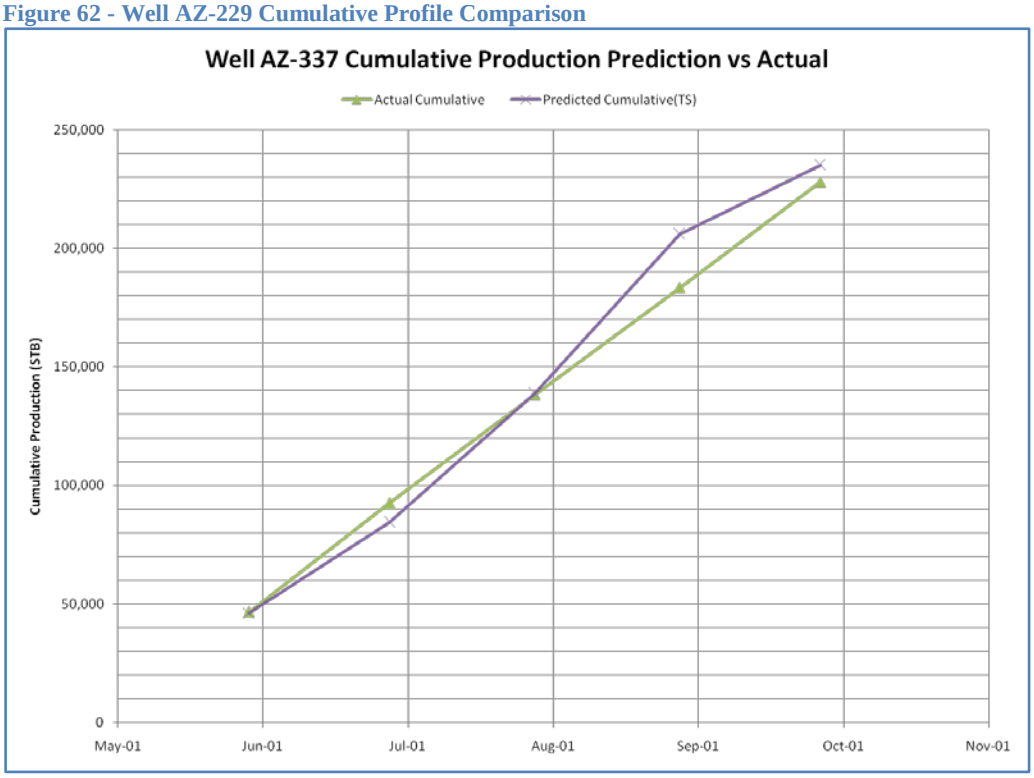

Figure 63 - Well AZ-337 Cumulative Profile Comparison

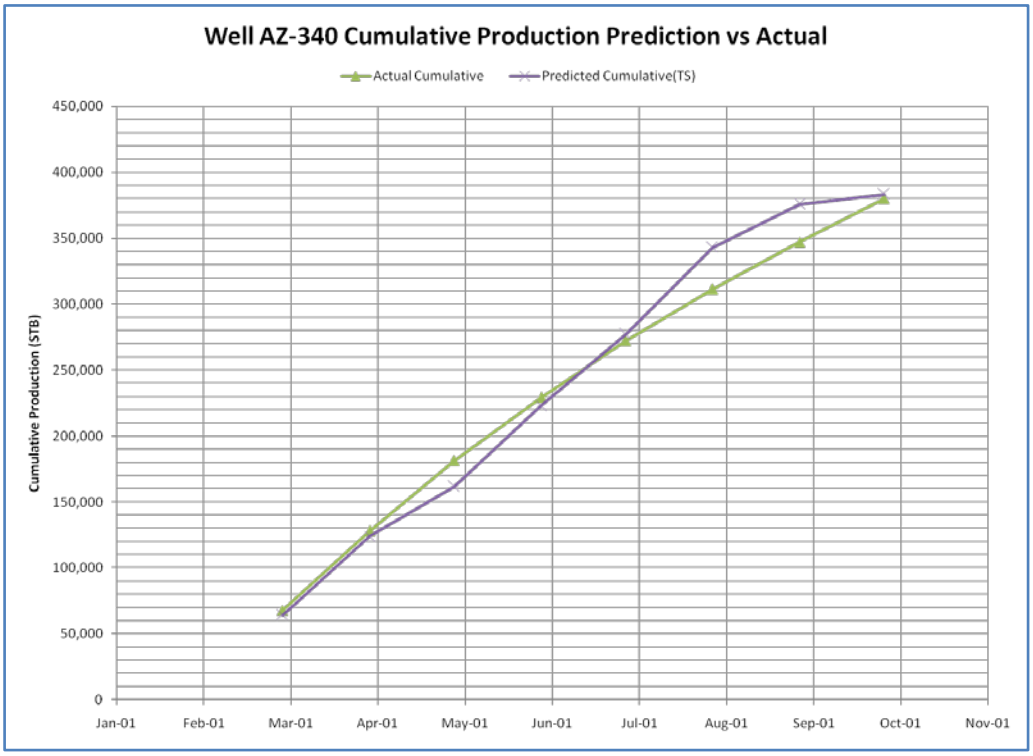

Figure 64 - Well AZ-340 Cumulative Profile Comparison

As it is visible in three out of four wells a fairly good prediction of cumulative production is obtained. The error distribution is presented in Figure 65.

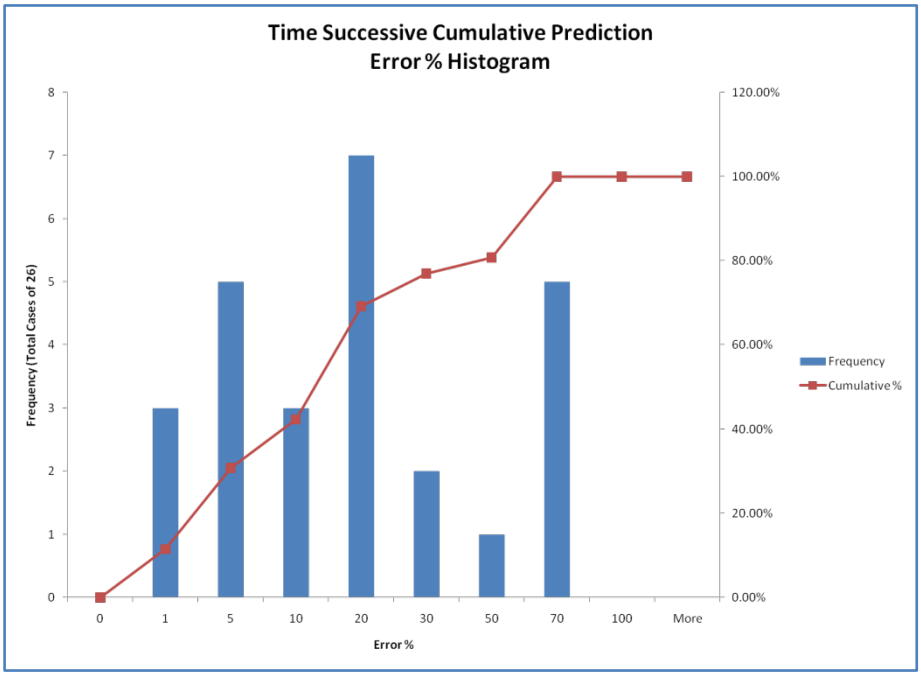

Figure 65 - Time Successive Prediction - Error Distribution

5. Conclusions and Discussions

This work was dedicated to a formal presentation of the concept of spatio-temporal data driven modeling technique and it's applicability to production data analyses. In this study we presented a new workflow for production prediction. It was shown that incorporating the spatio-temporal dependencies of fluid flow in the porous media and its footprints in production data enables us to build a field-wide model from multiple, individual single-well models. These spatial and temporal dependencies are addressed by incorporating the information content of the closest offset wells in the model.

Geostatistics methods provide a full field perception of the geological characteristics that is used in developing the field-wide model. In this approach the field-wide comprehension of the reservoir behavior is accomplished from single-well production data analysis. The Voronoi delineation of the reservoir gives a better spatial definition to the single wells analysis. By estimating this ultimate drainage area the original hydrocarbon in place for each well is also predictable. Even though this may not project the exact amount of reserve surrounding each well; it gives us an understanding of well's future performance.

Intelligent, Time-Successive Production Modeling (ITSPM) was successfully applied to a synthetic reservoir and a real field. Results for both cases show promising future for this technique. It is important to note that this work is one more step in the overall objective of developing data driven empirical reservoir models.

6. Appendix (A) - Geostatistical Analysis

To model the characteristics throughout the entire reservoir Ordinary Kriging was used to generate the map. The course of action for this mapping starts with modeling the Semivariogram of each parameter in the reservoir based on available data points at well location. Once a semivariogram is found for each parameter; the Ordinary Kriging algorithm is utilized to find the parameter values at all locations in the field.

Here a brief description about semivariogram calculation and the algorithm used for ordinary Kriging is provided.

6.1. Semi-Variogram and Model Prediction

Definition: "Semivariogram is a statistic that assesses the average decrease in similarity between two random variables as the distance between the variables increases".

In geostatistics semivariogram is a powerful tool to predict the spatial dependencies. It's used more than covariance in Kriging. There are a couple of reasons for this preference. Some of them are listed in below.

1. There is no need to know the Random Function's mean to be able to calculate or (estimate) the Semivariogram.

2. Existence of Semivariogram requires less strict assumptions than covariance.

3. Adding a constant to the random function does not change its Semi-Variogram.

4. Estimating the Semivariogram is easier than of a Covariance, in presence of a drift.

General definition of semivariogram is (20)

$$\gamma(x,y) = \frac{1}{2}E(|Z(x) - Z(y)|^2)$$

Where *E* (.) is the expected value function (21) and *Z* (.) can represent any of the reservoir characteristics at different locations in the field.

Under second order stationary assumption (20) and presuming a constant value for *E* (*Z* (.)) the definition becomes as following

$$\gamma(x,y) = \frac{1}{2}Var(|Z(x) - Z(x+h)|^2)$$

Now we can assume that variogram is not a function of the location but only a function of the distance between two locations namely *h* that from now we call it lag.

6.1.1. Experimental Semivariogram

Semivariogram is not the easiest statistic measurement to calculate. The simplest way to calculate it is based on the data we have is called an Experimental Semivariogram:

$$\gamma(x,y) = \frac{1}{2n(h)}\sum_{i=1}^{n(h)}(|Z(x_i) - Z(x_i+h)|^2)$$

Where *n* (*h*) is the number of pairs of data points at distance *h* apart.

There are some problems concerned with the experimental Variogram:

1. The estimation is not robust with respect to outliers.

2. There is a dubious assumption with this method: "one realization is sufficient to determine properties of the ensemble of all possible realization" by this we totally ignore that our data is a partial realization of the main random function and is insufficient to deduce that for sure.

3. We are assuming an intrinsic stationary random function. This results in semivariogram being only a function of the lag and is only true if the mean is constant. This causes us a problem when data exhibit a drift (a gentle and systematic variation in

the mean) in this case at first, one should remove the drift from the data and then calculate the semivariogram of the residuals.

As you may notice the estimation accuracy is directly proportional to the number of pairs. It is clear the larger the lag is the fewer the number of the pairs for a given distance will be. In Kriging the part of the semivariogram which is close to the origin requires the most accurate estimation because of its higher influence on the results. A rough rule is to limit the estimation to lags with a minimum of 30 pairs (20).

6.1.2. Semi-Variogram Models

Different models are used to be fitted to the experimental semi-variogram information. These are predefined deterministic functions that are fitted to the experimental data by using a minimum least square error technique.

Spherical Semi-Variogram

$$\gamma(h) = \begin{cases} C\left(\frac{3h}{2a} - \frac{1}{2}\frac{h^3}{a}\right) & 0 \le h \le a \\ C & a \le h \end{cases}$$

Exponential Semi-Variogram

$$\gamma(h) = C(1 - e^{\frac{-3h}{a}})$$

Gaussian Semivariogram

$$\gamma(h) = C(1 - e^{-3(\frac{h}{a})^2}$$

Power Semi-Variogram

$$\gamma(h) = \alpha h^{\beta}$$

Pure Nugget Effect Semi-Variogram

$$\gamma(h) = \begin{cases} 1 & h = 0 \\ 0 & O.W. \end{cases}$$

6.2. Kriging

Kriging is a spatial interpolation technique. It was first developed by the French mathematician Georges Matheron (22), based on the Master's thesis of Daniel Grehardus Krige.

The method is a linear least squares estimation. It is said to be linear since the estimator is a linear combination of the known values of the Random Function in the sampled points.

Kriging brings the best linear unbiased estimation, based on a stochastic model of the spatial dependence defined either by the Semivariogram or by known mean and Covariance.

In general form Kriging estimator, calculates the Random Function at the desired location based on the sample set, by assigning weight factors to each sample.

$$\hat{Z}(x_0) = \sum_{i=1}^{n} \lambda_i(x_0) Z(x_i)$$

Where λ_is are the weight factors associated with each data point.

Like all types of estimations, there is an error associated with this method. The error is defined as the variance of the estimated value and the exact value.

$$\sigma_k^2(x_0) = Var\left[\hat{Z}(x_0) - Z(x_0)\right]$$
$$= \sum_{i=1}^{n}\sum_{j=1}^{n} \lambda_i(x_0)\lambda_j(x_0) Cov\left(x_i, x_j\right) + Var\left(Z(x)\right)$$
$$- 2\sum_{i=1}^{n} \lambda_i(x_0)\, Cov(x_i, x_0)$$

The estimator minimizes this variance by choosing the weight factors in the estimator equation.

A set of constraints are introduced into the weight optimization process so the estimator remains unbiased that is honoring the actual point values at data points.

$$E\left[\hat{Z}(x) - Z(x)\right] = \sum_{i=1}^{n} \lambda_i(x_0)\mu(x_i) - \mu(x_0)$$

Where $\mu(x_i)$ are the Lagrange multipliers for the constrained optimization process.

6.2.1. Ordinary Kriging

Ordinary Kriging is used in cases that the expected value of the attribute which being kriged is unknown. So the estimator will be

$$\hat{Z}(x_0) = \sum_{i=1}^{n} \lambda_i(x_0)Z(x_i)$$

And for satisfying the unbiased constraint

$$\sum_{i=1}^{n} \lambda_i = 1$$

We assume the attribute we are performing the Kriging on honor the intrinsic hypothesis over the sampling domain (Intrinsic Random Function) (20). This implies that

$$E[Z(x)] = m \quad \{Contant\ mean\ value\}$$

$$Var[Z(x) - Z(x+h)] = 2\gamma(h)$$

Where $\gamma(h)$ is the Semi-Variogram of the attribute. Semi-Variogram function correlates with covariance of the attribute as follow:

$$\gamma(h) = Cov(0) - Cov(h)$$

So finding one will result in having the other one available.

In this form of Kriging by holding the intrinsic random function assumption the estimation error will be as following

$$\sigma^2(x_0) = 2\sum_{i=1}^{n}\lambda_i\gamma(x_i - x_0) - \sum_{i=1}^{n}\sum_{j=1}^{n}\lambda_i\lambda_j\gamma(x_i - x_j)$$

Algorithm used for Ordinary Kriging

In order to perform the algorithm some matrices and vectors are calculated or defined as following

Covariance Matrix of the attribute is calculated within the sampled data set. This can be done by modeling the Semi-Variogram and calculating the covariance for all "lag" values. matrix G is constructed as follows

$$G = \begin{pmatrix} Cov(x_j - x_i) & 1 \\ 1 & 0 \end{pmatrix}_{i,j=1:n}$$

Weight factors vector is defined

$$L = [\lambda_i, -\mu]'_{i=1:n}$$

Covariance Vector of the attribute between data points and the estimation location is defined

$$v = [Cov(x_0 - x_i), 1]'_{i=1:n}$$

The attribute data points vector is also defined

$$Z = [Z(x_i), 0]_{i=1:n}$$

Now that all the definitions are made the algorithm is designed and implemented in Visual Basic environment.

Calculate *V*

Calculate *v*

Solve *VL=v*

Find the estimate value

$\hat{Z}_{OK}(x_0) = Z'L = Z'^{V^{-1}}v$

Calculate the ordinary Kriging estimation variance

$\sigma^2_{OK}(x_0) = Cov(0) - v'L = Cov(0) - v'V^{-1}v$

7. Bibliography

1. **Gomez, Y. , Khazaeni, Y. , Mohaghegh, S.D.** Top-Down Intelligent Reservoir Modeling (TDIRM). *SPE Annual Technical Conference and Exhibition.* 2009.

2. **Mohaghegh, S.D.** Top-Down Intelligent Reservoir Modeling (TDIRM), a New Approach in Reservoir Modeling by Integrating Classic Reservoir Engineering with Artificial Intelligence and Data Mining (AI&DM). 2009.

3. **Arps, J.J.** Analysis of Decline Curves. *Trans, AIME.* 1945.

4. **Fetkovich M.J., Vienot M.E., Bradley M.D. , Kiesow U.G.** Decline Curve Analysis Using Type Curves - Case histories. *SPE Formation Evaluation.* December 1987.

5. **Hurst, William.** Water Influx Into a Reservoir and Its Application to the Equation of Volumetric Balance. *Petroleum Transactions, AIME.* 1943, Vol. 151.

6. **Hurst, W.** Unsteady Flow of Fluids in Oil Reservoirs. *Physics.* January 1934.

7. **Fetkovich, M.J.** Decline Curve analysis Using Type Curves. *Journal of Petroleum Technology.* June 1980.

8. **Carter, Robert D.** Charachteristic Behavior of Finite Radial and Linear Gas Flow Systems - Constant Terminal Pressure Case. *SPE/DOE Low Permeability Symposium.* May 1981.

9. **Fraim, M.L. , Wattenbarger R.A.** Gas Reservoir Decline-Curve analysis Using Type Curves With Real Gas Pseudopressure and Normalized Time. *SPE Formation Evaluation.* December 1987.

10. **Agarwal, R.G.** Real Gas Pseudo-time - A New Function for Pressure Buildup analysis of MHF Gas Wells. *SPE Annual Conference and Exhibition.* 1979.

11. **Lee, W.J. , Holditch, S.A.** Application of Pseudotime to Buildup Test Analysis of Low-Permeability Gas Wells With Long-Duration Wellbore Storage Distortion. *JPT.* December 1982.

12. **Palacio, J.C. , Blasingame, T.A.** Decline-Cruve Analysing Using Type Curves - Analysis of Gas Well Prodcution Data. *SPE Joint Rocky Mountain Regional and Low Permeability Reservoirs Symposium.* April 1993.

13. **Lee, W.J. , Wattenbarger, R.A.** *Gas Reservoir Engineering.* 1996. Vol. 5, SPE Textbook Series.

14. **Agarwal, R.G. , Gardner D.C. , Kleinsteiber S.W., Fussell D.D.** Analysing Well Production Data Using Combined Type Curve and Decline Curve Analysis Concepts. *SPE Reservoir Eval. & Eng.* October 1999, Vol. 5.

15. **Cox, S.A. , Gilbert, J.V. , Sutton, R.P. , Ronald, P.S.** Reserve Analysis for Tight Gas. *SPE Eastern Regional Meeting.* 2002.

16. **Gaskari, R. , Mohaghegh, S.D.** An Integrated Technique for Production Data Analysis with Application to Mature Fields. *SPE Gas Technology Symposium.* 2006.

17. **Shepard, D.** A two-dimensional interpolation function for irregularly-spaced data. *23rd ACM National Conference.* 1968.

18. **Ledoux, H. , Gold, C.** *An Efficient Natural Neighbout Interpolation Algorithm for Geoscientific Modeling.* Department of Land Surveying and Geo-Informatics, Hong Kong Polytechnic University. Hong Kong : s.n.

19. **Mohaghegh, S.D.** http://www.intelligentsolutionsinc.com/. [Online]

20. **Olea, R.A.** *Geostatistics for Engineers and Earth Sceintists.* s.l. : Kluwer Academics Publishers, 1999.

21. **WIKIPEDIA.** http://en.wikipedia.org/wiki/Expected_value. [Online]

22. **Matheron, G.** *The Theory of Regionalized Variables and Its Application.* s.l. : The Ecole Nationale Superieure des Mines de Paris, 1971.

23. **Mattar L., Anderson D.M.** A systematic and Comprehensive Methodology for Advanced Analysis of Production Data. *SPE Technical Conference and Exhibition.* Oct 5-8, 2003.

24. **Anderson D.M., Stotts G.W.J. , Mattar L., Ilk D., Blasingame T.A.** Production Data analysis - Challenges, Pitfalls, Diagnostic. *SPE Annual technical Conference and Exhibition.* September 24-27, 2006.

25. **A.G., Journel.** *Fundamentals of Geostatistics in Five Lessons.* s.l. : Maria Luisa Crawford and Elaine Padovani, 1989.